

Supporting Information

Exploring the Impact of Ring Mobility on the Macroscopic Properties of Doubly Threaded Slide-Ring Gel Networks

*J. Oh, G. Liu, H. Kim, J. E. Hertzog, N. Nitta, S. J. Rowan**

Exploring the Impact of Ring Mobility on the Macroscopic Properties of Doubly Threaded Slide-Ring Gel Networks

Authors: Jongwon Oh^{a†}, Guancen Liu^{b†}, Hojin Kim^{ac}, Jerald E. Hertzog^a, Natsumi Nitta^a, and Stuart J. Rowan^{*abd}

a Pritzker School of Molecular Engineering, University of Chicago, Chicago, IL 60637, USA

b Department of Chemistry, University of Chicago, Chicago, IL 60637, USA

c James Franck Institute and Department of Physics, University of Chicago, Chicago, IL 60637, USA.

d Chemical Science and Engineering Division and Center for Molecular Engineering, Argonne National Laboratory, 9700 S. Cass Ave., Lemont, IL 60434, USA

† These authors contributed equally

Materials and Methods <ul style="list-style-type: none"> • <u>Materials</u> • <u>Instruments and Methods</u> 	Pages 2-3
Synthesis of thread and macrocycles <ul style="list-style-type: none"> • <u>Synthesis of Nonaethylene glycol monotosylate</u> • <u>Synthesis of photo-curable thread 1</u> • <u>Synthesis of macrocycle 2⁵⁶</u> • <u>Synthesis of macrocycle 2⁴⁶</u> • <u>Synthesis of macrocycle 2⁶⁸</u> 	Pages 4-10 <ul style="list-style-type: none"> • Fig. S1 • Figs. S2-3 • Figs. S4-5 • Fig. S6 • Fig. S7
Synthesis of pseudo[3]rotaxane (P3R) and supramolecular crosslinkers <ul style="list-style-type: none"> • <u>UV/Vis titration of macrocycle 2⁵⁶</u> • <u>Synthesis of doubly threaded P3R crosslinker using 1, 2⁵⁶, and Zn(II)</u> • <u>Synthesis of doubly threaded P3R crosslinker using 1, 2⁴⁶, and Zn(II)</u> • <u>Synthesis of doubly threaded P3R crosslinker using 1, 2⁶⁸, and Zn(II)</u> • <u>Synthesis of 4-arm supramolecular crosslinker using 1 and Zn(II)</u> 	Pages 11-15 <ul style="list-style-type: none"> • Fig. S8 • Figs. S9-10 • Figs. S11-12 • Figs. S13-14 • Figs. S15-16
Fabrication of doubly threaded slide-ring gel networks (dt-SRGs), entangled gel network (EG), and covalent gel network (CG)	Pages 16-17
Characterization of dt-SRGs, EG, and CG <ul style="list-style-type: none"> • <u>UV-Vis absorbance, fluorescence spectra of dt-SRG upon demetalation</u> • <u>FT-IR spectra of dt-SRG</u> • <u>NMR study for the calculation of ring content within dt-SRGs</u> • <u>Gel fraction of dt-SRG 3⁵⁶_{3/97}, EG 4_{3/97}, and CG 5_{3/97}</u> • <u>Differential scanning calorimetry (DSC) measurement</u> • <u>UV-Vis, fluorescence spectra of dt-SRGs upon remetalation</u> • <u>Viscoelastic and macroscopic stress relaxation properties of dt-SRG 3⁵⁶_{3/97}, EG 4_{3/97}, and CG 5_{3/97}</u> 	Pages 18-26 <ul style="list-style-type: none"> • Fig. S17 • Fig. S18 • Figs. S19-22 • Fig. S23 • Fig. S24 • Fig. S25 • Fig. S26-27
Fabrication and characterization of dt-SRGs with different ring sizes <ul style="list-style-type: none"> • <u>Gel fraction and ring content of dt-SRGs 3⁴⁶_{3/97}, 3⁵⁶_{3/97}, 3⁶⁸_{3/97}</u> • <u>Swelling, viscoelastic, and macroscopic stress relaxation properties of dt-SRGs 3⁴⁶_{3/97}, 3⁵⁶_{3/97}, 3⁶⁸_{3/97}</u> • <u>DOSY spectra and diffusion coefficients of macrocycles</u> 	Pages 27-32 <ul style="list-style-type: none"> • Figs. S28-29 • Figs. S30-32 • Figs. S33-35
References	Page 33

Materials and Methods

Materials

All chemicals were purchased from Sigma-Aldrich and utilized without further purification, except where specified. Chromatography solvents were sourced from Fisher Scientific. Zinc di[bis(trifluoromethylsulfonyl)imide] was obtained from Strem Chemicals and stored in a nitrogen desiccator. Thymol standard for NMR TraceCERT® was acquired from Sigma-Aldrich and stored in a nitrogen desiccator. Nonaethylene glycol was purchased from AA Blocks. Poly(ethylene glycol) methyl ether acrylate ($M_n = 480 \text{ gmol}^{-1}$) and 4-arm PEG acrylate ($M_n = 2000 \text{ gmol}^{-1}$) were purchased from Sigma-Aldrich and creative PEGWorks, respectively. The synthesis of 2,6-bis(*N*-alkyl-benzimidazolyl)pyridine ligands was conducted according to previously reported literature procedures^[1-3]. 1H,1H,2H,2H-perfluoro octyl trichlorosilane (PFOTS) was purchased from AA Blocks. Deuterated solvents were purchased from ACROS Organics and Sigma-Aldrich. Tetrahydrofuran (THF) was dried over sodium and benzophenone. Dichloromethane was distilled over calcium hydride. Dimethylformamide (DMF) was dried with activated 4Å molecular sieves. All synthesized components were stored in a freezer at -40°C prior to use.

Instruments and Methods

Nuclear Magnetic Resonance Spectroscopy (NMR): NMR experiments were conducted utilizing a Bruker Ascend AVANCE III 500 MHz spectrometer (126 MHz for C^{13}), a Bruker AVANCE II+ 500 MHz spectrometer (126 MHz for C^{13}), or a Bruker DRX 400 MHz spectrometer (101 MHz for C^{13}) at the University of Chicago Chemistry Department's NMR Facility. ^1H NMR spectra were referenced to the residual protonated solvent signal, and ^{13}C NMR spectra were referenced to the deuterated solvent carbon resonance signal.

Diffusion-ordered NMR Spectroscopy (DOSY NMR): DOSY NMR experiments were carried out with dilute solutions in 5mm NMR tubes at 25°C using the 2D Bruker pulse program `dstebpgp3s`^[4,5], which incorporates a double stimulated echo for convection compensation, a longitudinal echo delay, bipolar gradient pulses, and three spoil gradients. The corresponding 1D pulse sequence `dstebpgp3d1d` was employed to optimize the parameters D20 (“big delta”, the major diffusion delay) and P30 (“little delta”, the diffusion gradient length), following the manufacturer-recommended method^[6]. Data acquisition involved a linear array of 32 diffusion gradient strengths (GPZ6 values) from 5% to 95%.

Matrix-Assisted Laser Desorption/Ionization Time-of-Flight Mass Spectrometry (MALDI-TOF MS): MALDI-TOF MS analyses were performed on a Bruker autoflex max MALDI-TOF spectrometer at the University of Chicago Mass Spectrometry Facility in linear mode using a dithranol as the matrix and sodium trifluoroacetate as the ionizer (or no ionizer).

UV-Vis Spectrometry: UV-Vis spectra were recorded using a Shimadzu UV-3600 Plus UV-Vis-NIR spectrophotometer equipped with a 1 cm width quartz cuvette or a quartz glass slide. Solution samples were prepared with a 1 cm width quartz cuvette. Gels (fully swollen in propylene carbonate) were cut into a circular shape (diameter: 10mm) and placed onto a quartz glass slide.

Fluorescence Spectrometry: Fluorescence spectra were measured using a Duetta 3-in-1 spectrofluorometer (HORIBA Scientific). Gels (fully swollen in propylene carbonate) were cut into a circular shape (diameter: 10mm) and placed onto a quartz glass slide.

FT-IR Spectrometry: FT-IR spectra were recorded using a Shimadzu IRTracer-100 FT-IR with ATR diamond in the Soft Matter Characterization Facility at the University of Chicago. dt-SRGs films (before and after demetallation) were prepared for these measurements.

Differential Scanning Calorimetry (DSC): DSC measurements were conducted using a TA Instruments Discovery 2500 Differential Scanning Calorimeter in the Soft Matter Characterization Facility at the University of Chicago. dt-SRGs, EG, and CG films were prepared in aluminum Tzero pans from TA Instruments and were sealed. Typical test conditions involved a heat-cool-heat procedure (200°C/-90°C/200°C) executed at a rate of 10°C/min with a 5 min isotherm between each ramp.

Oscillatory Compression Rheology: Oscillatory compression rheology experiments were performed using a TA Instruments RSA G2 with the 12 mm compression plate geometry. Gel samples (fully swollen in propylene carbonate) were cut using a 10 mm die punch and preloaded with 0.15 N to ensure uniform contact between the sample and plates. Frequency sweeps were performed from 1000 rad/s to 0.01 rad/s with a strain amplitude of 1%.

Compressive Stress Relaxation: Compressive stress relaxation experiments were carried out using a TA Instruments RSA G2 with the 12 mm compression plate geometry. Gel samples (fully swollen in propylene carbonate) were cut using a 10 mm die punch and preloaded with 0.15 N to ensure uniform contact between the sample and plates. An instantaneous strain of 4% was applied.

Synthesis of thread and macrocycles

Synthesis of Nonaethylene glycol monotosylate

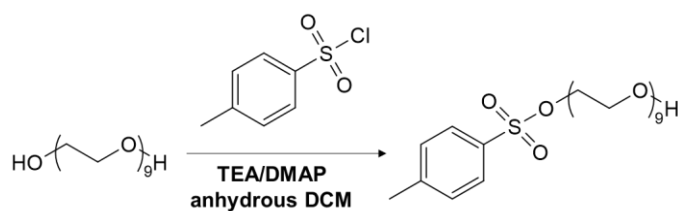


Figure S1. Synthesis of Nonaethylene glycol monotosylate.

Nonaethylene glycol (25.0 g, 60.3 mmol), triethylamine (TEA) (5.88 mL, 42.2 mmol), and 4-dimethylaminopyridine (DMAP) (0.245 g, 2.01 mmol) were placed in a flame-dried two-neck round-bottom flask under an argon atmosphere, and anhydrous dichloromethane (DCM) (220 mL) was added. The mixture was cooled to 0°C in an ice-water bath. 4-Toluenesulfonyl chloride (TsCl) (6.14 g, 32.2 mmol) in anhydrous DCM (90 mL) was added dropwise to the reaction mixture over 16 hours using a syringe pump. Following this addition, the ice-bath was removed, and the reaction mixture was warmed to room temperature and allowed to stir for another 8 hours. The reaction mixture was then diluted with DCM (200 mL) and washed with brine (1 × 500 mL). The organic layer was separated. The aqueous layer was then extracted with DCM (3 × 300 mL). The organic layers were combined, dried with sodium sulfate, filtered, and the solvent was removed in vacuo. The resulting oil was purified by silica gel chromatography (0-10% methanol in ethyl acetate) to yield mono-tosylated nonaethylene glycol as a clear oil (12.3 g, 21.6 mmol, 67% isolated yield). ¹H NMR (500 MHz, CDCl₃) δ 7.80 (d, J = 8.1 Hz, 2H), 7.34 (d, J = 8.0 Hz, 2H), 4.16 (t, J = 4.8 Hz, 2H), 3.74 – 3.56 (m, 34H), 2.78 (t, J = 6.2 Hz, 1H), 2.45 (s, 3H). ¹³C NMR (126 MHz, CDCl₃) 144.61, 133.09, 129.89, 128.03, 72.62, 70.80, 70.67, 70.62, 70.61, 70.59, 70.57, 70.39, 69.32, 68.73, 61.77, 21.70. MALDI-TOF MS ([M]⁺Na⁺): found *m/z* 591.13 (C₂₅H₄₄ NaO₁₂S calcd. for *m/z* 591.25)

Synthesis of photo-curable thread **1**

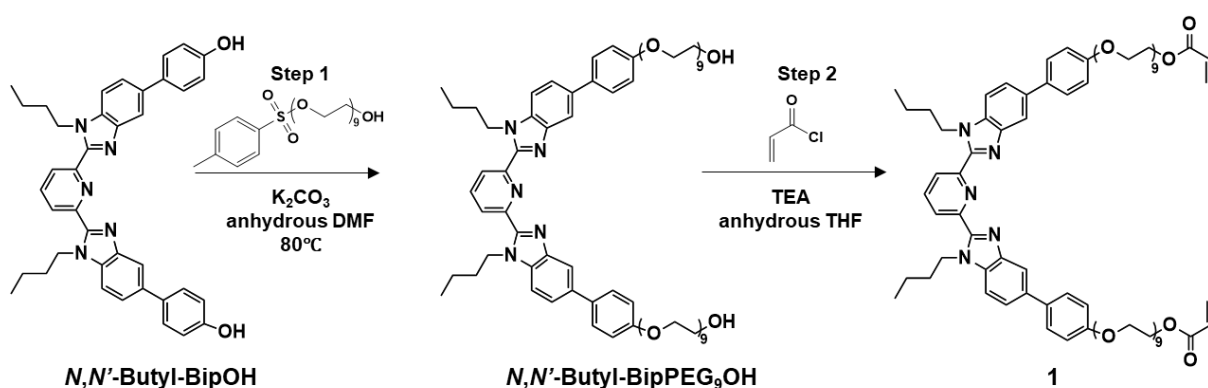


Figure S2. Synthesis of **1**.

Step 1: 2,6-Bis(1'-butyl-5'-(4''-hydroxy)phenylbenzimidazol-2'-yl)pyridine (*N,N'*-Butyl-BipOH)^[2] (2.43 g, 4.00 mmol), mono-tosylated nonaethylene glycol (5.68 g, 10 mmol) and cesium carbonate (Cs_2CO_3) (5.21 g, 16.0 mmol) were placed in a flame-dried two-neck round-bottom flask under argon atmosphere and anhydrous DMF (15 mL) was added. The mixture was heated to 75 °C for 16 h. The solvent was removed in vacuo. The residue was dissolved in chloroform, and the residual salt was removed by filtration. The chloroform was washed with brine (1 × 500 mL). The organic layer was separated. The aqueous layer was then extracted with DCM (5 × 200 mL). The organic layer and the DCM extractions were combined, dried with sodium sulfate, filtered, and the solvent was removed in vacuo. The oil was purified by silica gel chromatography (0-10% methanol in chloroform) to yield *N,N'*-Butyl-BipPEG₉OH as a white solid (4.20 g, 3.00 mmol, 75% isolated yield). ¹H NMR (500 MHz, $CDCl_3$) δ 8.34 (d, 2H), 8.07 (t, $J = 7.9$ Hz, 1H), 8.01 (d, $J = 7.7$ Hz, 2H), 7.63 – 7.52 (m, 6H), 7.50 (d, $J = 8.5$ Hz, 2H), 7.03 (d, $J = 8.2$ Hz, 4H), 4.76 (t, $J = 7.3$ Hz, 4H), 4.20 (t, $J = 5.0$ Hz, 4H), 3.90 (t, $J = 5.0$ Hz, 4H), 3.81 – 3.55 (m, 64H), 1.75 (t, $J = 7.7$ Hz, 4H), 1.14 (h, $J = 7.1$ Hz, 4H), 0.73 (t, 6H). ¹³C NMR (126 MHz, $CDCl_3$) 158.19, 150.75, 150.03, 143.44, 138.26, 136.17, 135.53, 134.49, 128.40, 125.59, 123.17, 118.10, 115.08, 110.54, 72.63, 70.91, 70.91, 70.70, 70.66, 70.64, 70.62, 70.61, 70.59, 70.38, 69.83, 67.62, 61.73, 44.83, 32.23, 19.92, 13.57. MALDI-TOF MS ($[M]+H^+$): found m/z 1400.32 ($C_{75}H_{110}N_5O_{20}$ calcd. for m/z 1400.77).

Step 2: *N,N'*-Butyl-BipPEG₉OH (1.00 g, 0.71 mmol) and triethylamine (0.18 g, 1.78mmol) were placed in a round-bottom flask purged with argon, and anhydrous THF (30 mL) was added. Acryloyl chloride (0.16 g, 1.78mmol) was then added dropwise to the flask, and the mixture was stirred for 6 hours. Afterward, THF was removed in vacuo. The resulting residue was then dissolved in ethyl acetate and extracted using water three times, followed by drying with $MgSO_4$. Insoluble materials were filtered off, and the filtrate was further purified by silica gel

chromatography (0-2% methanol in chloroform) to yield a light yellow solid, **1** (0.56g, 0.37mmol, isolated yield 52%). ¹H NMR (500 MHz, CDCl₃) δ 8.34 (d, *J* = 7.9 Hz, 2H), 8.07 (t, *J* = 7.9 Hz, 1H), 8.02 (d, *J* = 1.6 Hz, 2H), 7.63 – 7.54 (m, 6H), 7.49 (d, *J* = 8.5 Hz, 2H), 7.05 – 7.00 (m, 4H), 6.42 (dd, *J* = 17.3, 1.5 Hz, 2H), 6.14 (dd, *J* = 17.3, 10.4 Hz, 2H), 5.82 (dd, *J* = 10.4, 1.5 Hz, 2H), 4.76 (t, *J* = 7.3 Hz, 4H), 4.33 – 4.28 (m, 4H), 4.19 (t, *J* = 4.9 Hz, 4H), 3.89 (t, *J* = 4.9 Hz, 4H), 3.83 – 3.43 (m, 56H), 1.79 – 1.69 (m, 4H), 1.13 (dt, *J* = 16.9, 7.5 Hz, 4H), 0.72 (t, *J* = 7.4 Hz, 6H). ¹³C NMR (101 MHz, CDCl₃) δ 166.21, 158.16, 150.70, 149.95, 143.34, 138.27, 136.20, 135.47, 134.47, 131.05, 128.39, 128.30, 125.59, 123.18, 118.04, 115.04, 110.52, 70.88, 70.67, 70.64, 70.59, 69.81, 69.14, 67.58, 63.73, 50.83, 44.82, 32.20, 19.90, 13.54. MALDI-TOF MS ([M]+H⁺): found *m/z* 1509.28 (C₈₁H₁₁₄N₅O₂₂ calcd. for *m/z* 1508.80).

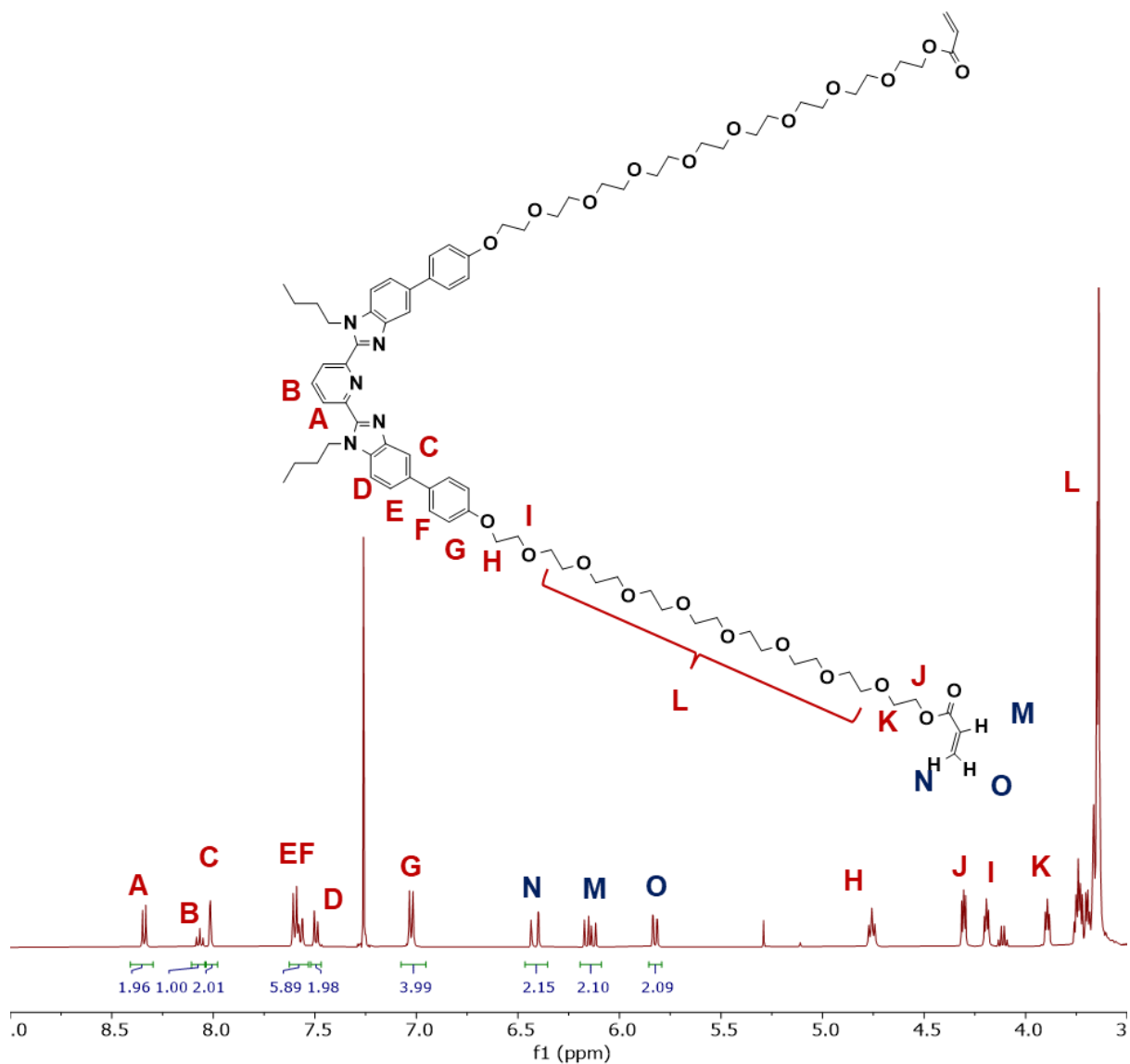


Figure S3. ¹H NMR spectrum of thread 1.

Synthesis of macrocycle **2⁵⁶**

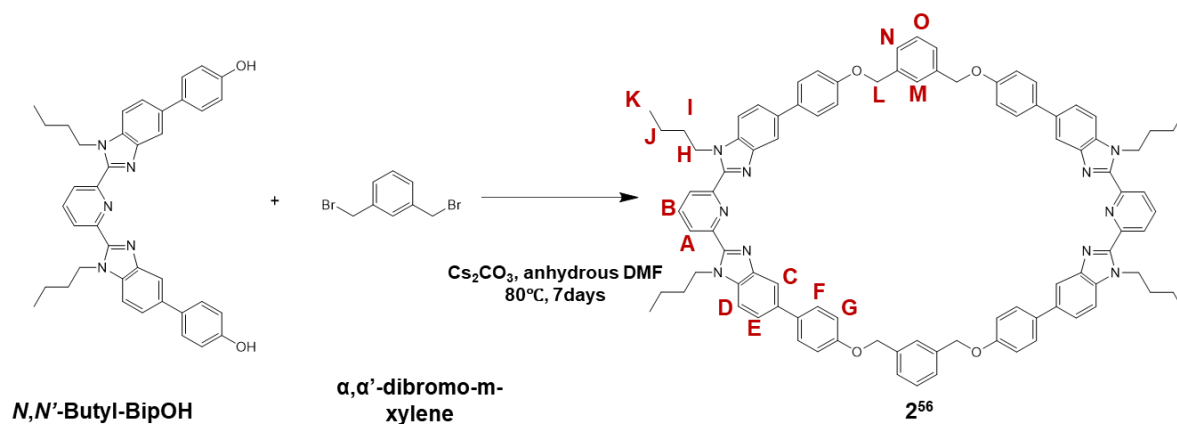


Figure S4. Synthesis of macrocycle **2⁵⁶**.

***N,N'*-Butyl-BipOH** (1.00 g, 1.65 mmol), Cs_2CO_3 (2.15 g, 6.6 mmol), and anhydrous DMF (206mL) were placed in a round-bottom flask purged with argon. α,α' -dibromo-*m*-xylene (0.435g, 1.65 mmol), and anhydrous DMF (206mL) were placed in a 500mL addition funnel purged with argon, and this mixture was added dropwise to the round-bottom flask over 3 days at 80°C. The resulting mixture was stirred at 80°C for an additional 4 days. DMF was subsequently removed under vacuum, and the residue was dissolved in hot chloroform. Insoluble materials were filtered off, and the filtrate was collected and purified by triethylamine-treated silica gel chromatography (0-1% methanol in chloroform), followed by recrystallization (chloroform/methanol mixture) to yield a white solid, **2⁵⁶** (0.18g, 0.123 mmol, isolated yield 15%). ¹H NMR (500 MHz, CDCl_3) δ 8.33 (d, $J = 7.8$ Hz, 4H), 8.03 (t, $J = 7.9$ Hz, 2H), 7.92 (d, $J = 1.6$ Hz, 4H), 7.50 (s, 2H), 7.42 – 7.29 (m, 18H), 7.15 (d, $J = 8.4$ Hz, 4H), 6.87 – 6.80 (m, 8H), 5.26 (s, 8H), 4.56 (t, $J = 7.2$ Hz, 8H), 1.59 – 1.50 (m, 8H), 0.94 (h, $J = 7.4$ Hz, 8H), 0.58 (t, $J = 7.3$ Hz, 12H). ¹³C NMR (126 MHz, CDCl_3) δ 157.27, 150.36, 150.13, 143.33, 138.15, 138.12, 136.03, 135.38, 134.32, 129.17, 128.16, 126.02, 125.61, 125.59, 123.33, 117.84, 116.10, 110.50, 69.80, 44.55, 32.12, 19.74, 13.50. MALDI-TOF MS ($[\text{M}] + \text{H}^+$): found m/z 1420.21 ($\text{C}_{94}\text{H}_{87}\text{N}_{10}\text{O}_4$ calcd. for m/z 1419.69).

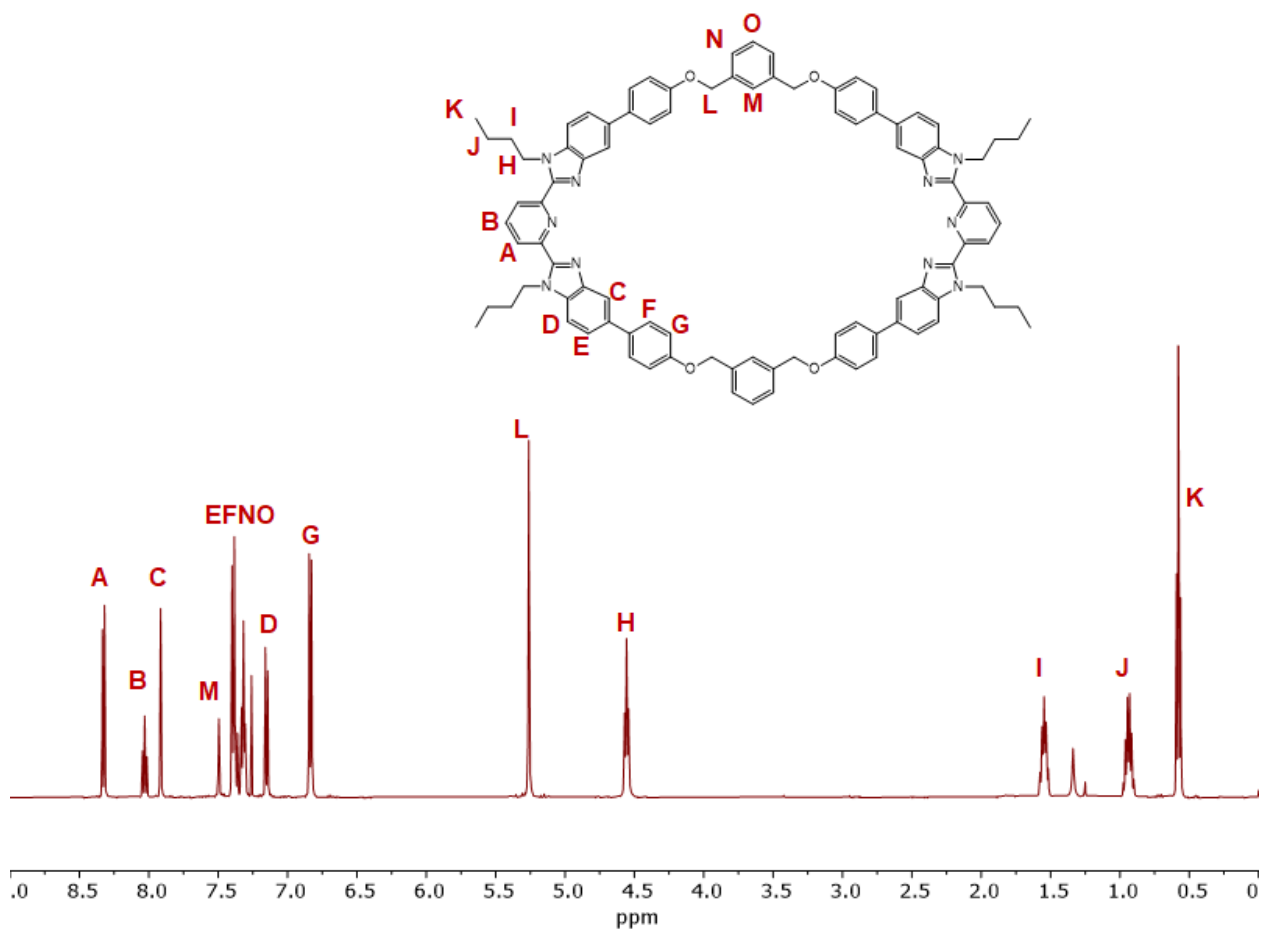


Figure S5. ^1H NMR spectrum of macrocycle **2⁵⁶**.

Synthesis of macrocycle **2⁴⁶**

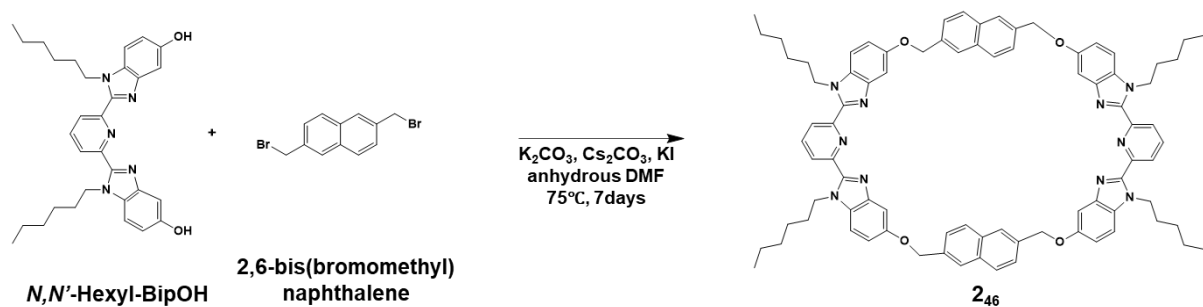


Figure S6. Synthesis of macrocycle **2⁴⁶**.

Potassium carbonate (K_2CO_3) (3.73 g, 27.0 mmol), Cs_2CO_3 (8.80 g, 27.0 mmol), potassium iodide (KI) (0.13 g, 0.785 mmol), and anhydrous DMF (500 mL) were placed in a round-bottom flask purged with argon. 2,6-bis(bromomethyl) naphthalene (0.35 g, 2.70 mmol), 2,6-Bis(1'-hexyl-5'-hydroxybenzimidazol-2'-yl)pyridine (*N,N'*-Hexyl-BipOH) (1.38 g, 2.70 mmol), and anhydrous DMF (500mL) were placed in a 500mL addition funnel purged with argon, and this mixture was added dropwise to the round-bottom flask over 2 days at 75°C.

The resulting mixture was stirred at 75°C for an additional 5 days. DMF was subsequently removed under vacuum, and the residue was dissolved in hot chloroform. Insoluble materials were filtered off, and the filtrate was collected and purified by triethylamine-treated silica gel chromatography (0-1% methanol in chloroform), followed by recrystallization (chloroform/methanol mixture) to yield a white solid, **2⁴⁶** (0.103 g, 0.077 mmol, isolated yield 5.7%). ¹H NMR and ¹³C NMR data were consistent with the previously reported compound³. MALDI-TOF MS ([M]+H⁺): found *m/z* 1327.84 (C₈₆H₉₁N₁₀O₄ calcd. for *m/z* 1327.72).

Synthesis of macrocycle **2⁶⁸**

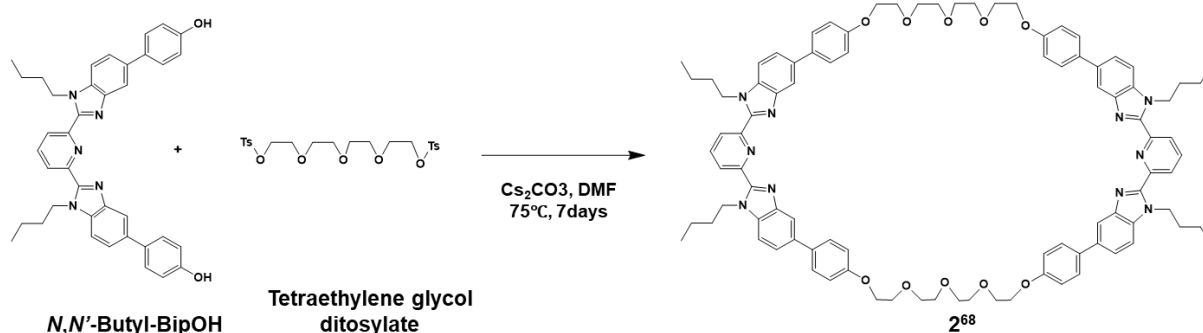


Figure S7. Synthesis of macrocycle **2⁶⁸**.

N,N'-Butyl-BipOH (2.12 g, 3.50 mmol), Cs₂CO₃ (4.56 g, 14.00 mmol), and anhydrous DMF (438mL) were placed in a round-bottom flask purged with argon. Tetraethylene glycol ditosylate (1.76 g, 3.50 mmol) and anhydrous DMF (438mL) were placed in a 500mL addition funnel purged with argon, and this mixture was added dropwise to the round-bottom flask over 2 days at 75°C. The resulting mixture was stirred at 75°C for an additional 5 days. DMF was subsequently removed under vacuum, and the residue was dissolved in hot chloroform. Insoluble materials were filtered off, and the filtrate was collected and purified by triethylamine-treated silica gel chromatography (0-2% methanol in chloroform), followed by recrystallization (chloroform/methanol mixture) to yield a white solid, **2⁶⁸** (0.06g, 0.039 mmol, isolated yield 2.2%). ¹H NMR and ¹³C NMR data were consistent with the previously reported compound². MALDI-TOF MS ([M]+H⁺): found *m/z* 1532.10 (C₉₄H₁₀₃N₁₀O₁₀ calcd. for *m/z* 1531.78).

Synthesis of pseudo[3]rotaxane (P3R) and supramolecular crosslinkers

UV/Vis titration of macrocycle 2^{56}

A solution of macrocycle 2^{56} at a concentration of $80\mu\text{M}$ was prepared using a solvent mixture of chloroform (CHCl_3) and acetonitrile (ACN) in a 3:2 ratio. Additionally, a 1 mM solution of $\text{Zn}(\text{NTf}_2)_2$ was prepared with the same CHCl_3 and ACN mixture and subsequently added to the solution of macrocycle 2^{56} , maintaining a consistent concentration of the macrocycle throughout the titration process. Initially, 2.5 mL (200nmol) of the macrocycle solution was dispensed into a 1 cm quartz cuvette, and its UV Vis spectrum was recorded. Subsequently, 40 μL (40 nmol) of the $\text{Zn}(\text{NTf}_2)_2$ solution was added to the cuvette, followed by another UV Vis spectrum measurement after a 5-minute interval. This sequential addition of $\text{Zn}(\text{NTf}_2)_2$ solution was repeated until an excess (greater than 4 mol equivalents) of $\text{Zn}(\text{NTf}_2)_2$ had been added to the system.

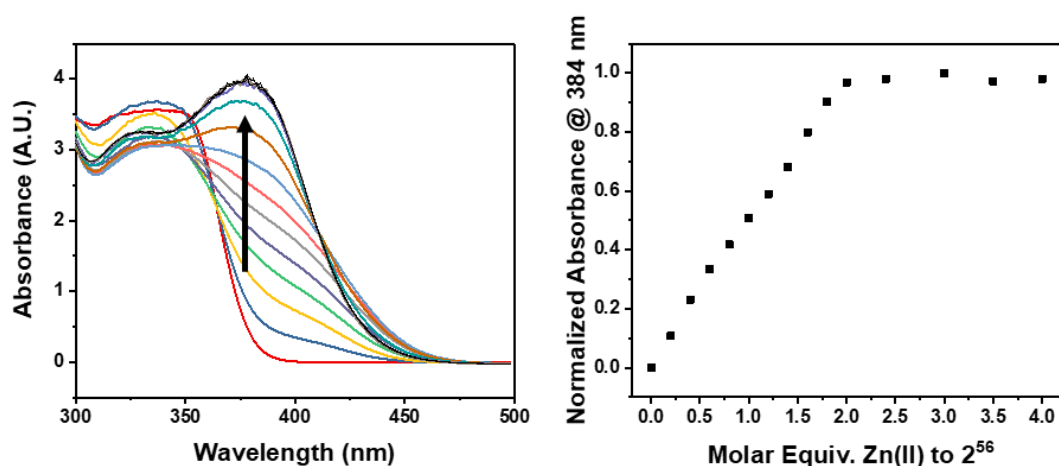


Figure S8. UV/Vis titration spectra (left) and absorbance at 384 nm (right) of 2^{56} with Zn^{2+} .

Synthesis of doubly threaded P3R crosslinker using **1**, **2⁵⁶**, and Zn(II)

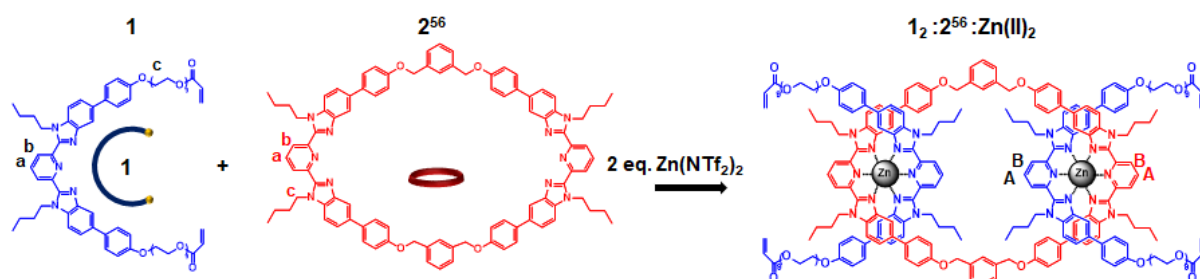


Figure S9. Synthesis of **2⁵⁶** based P3R crosslinker (**1₂:2⁵⁶:Zn(II)₂**).

A solution of macrocycle **2⁵⁶** (0.01g, 0.007 mmol) was prepared using 1.0 mL of CDCl₃, and a solution of thread **1** (0.021g, 0.014 mmol) was prepared using 0.5 mL of CDCl₃. While monitoring both N-CH₂ peaks on the alkyl groups of the Bip ligands, the thread solution was titrated into the macrocycle solution until a precise 2:1 ratio was achieved. A solution of Zn(NTf₂)₂ was prepared with a concentration of 20 mM using a mixture of CDCl₃ and d₃-MeCN. The Zn(NTf₂)₂ solution was added until all unbound free Bip peaks (a, b) around 8.04 and 8.33 ppm disappeared. In the NMR spectrum of the resulting P3R crosslinkers, the new peaks (A, B) around 8.73 and 9.05 ppm appeared, indicating that all Bip ligands are bound with Zn²⁺ ions in a 2:1 ratio.

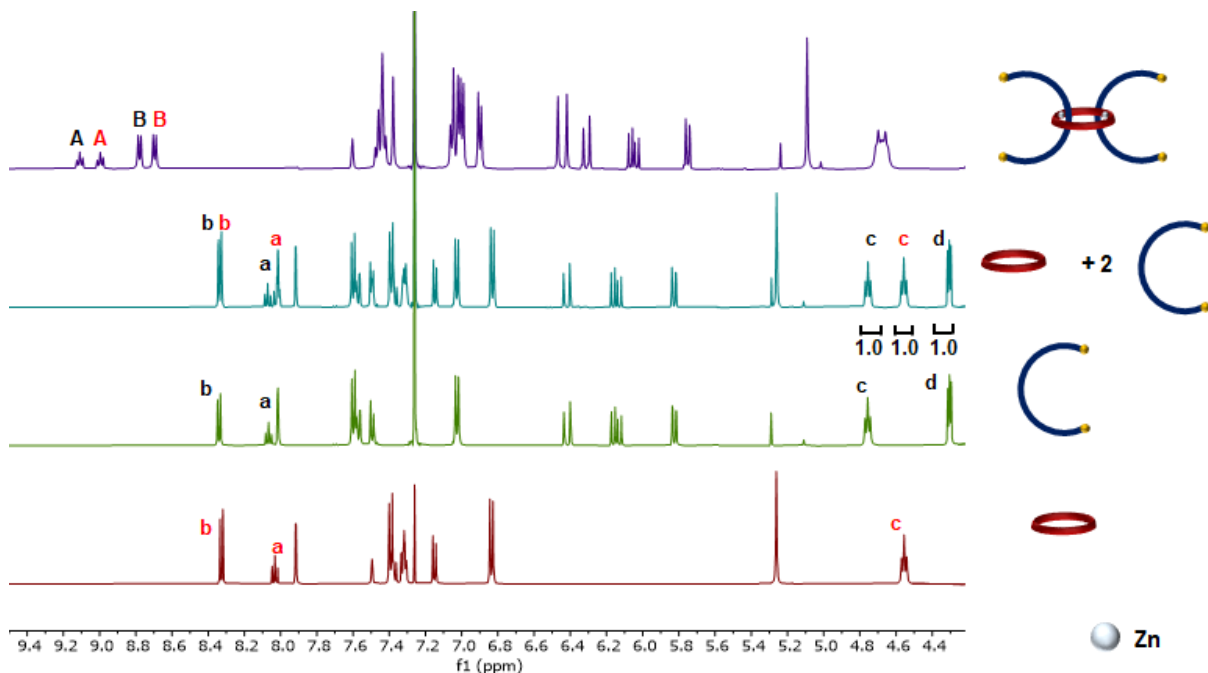


Figure S10. Partial ¹H NMR overlay (500 MHz, 25°C) of macrocycle **2⁵⁶**, thread **1**, the mixture of one **2⁵⁶** and two **1**, and **2⁵⁶** based P3R crosslinker (**1₂:2⁵⁶:Zn(II)₂**). ¹H assignments from Figure S9.

Synthesis of doubly threaded P3R crosslinker using **1**, **2⁴⁶**, and Zn(II)

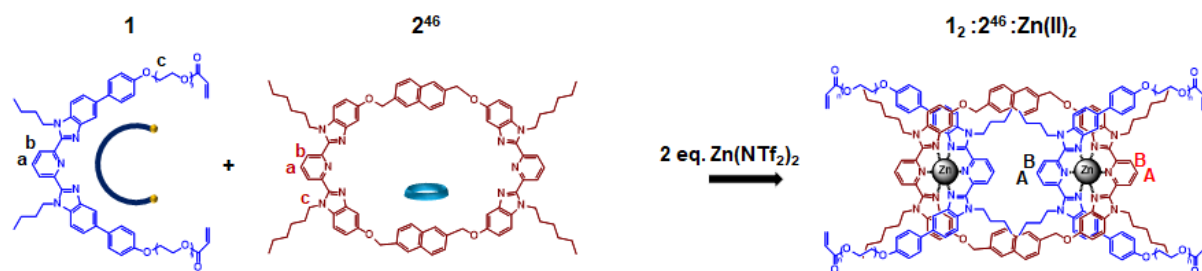


Figure S11. Synthesis of **2⁴⁶** based P3R crosslinker (**1₂:2⁴⁶:Zn(II)₂**).

A solution of macrocycle **2⁴⁶** (0.0093g, 0.007 mmol) was prepared using 1.0 mL of CDCl₃, and a solution of thread **1** (0.021g, 0.014 mmol) was prepared using 0.5 mL of CDCl₃. While monitoring both N-CH₂ peaks on the alkyl groups of the Bip ligands, the thread solution was titrated into the macrocycle solution until a precise 2:1 ratio was achieved. A solution of Zn(NTf₂)₂ was prepared with a concentration of 20 mM using a mixture of CDCl₃ and d₃-MeCN. The Zn(NTf₂)₂ solution was added until all unbound free Bip peaks (a, b) around 8.05 and 8.33 ppm disappeared. In the NMR spectrum of the resulting P3R crosslinkers, the new peaks (A, B) around 8.51, 8.73, and 9.10 ppm appeared, indicating that all Bip ligands are bound with Zn²⁺ ions in a 2:1 ratio.

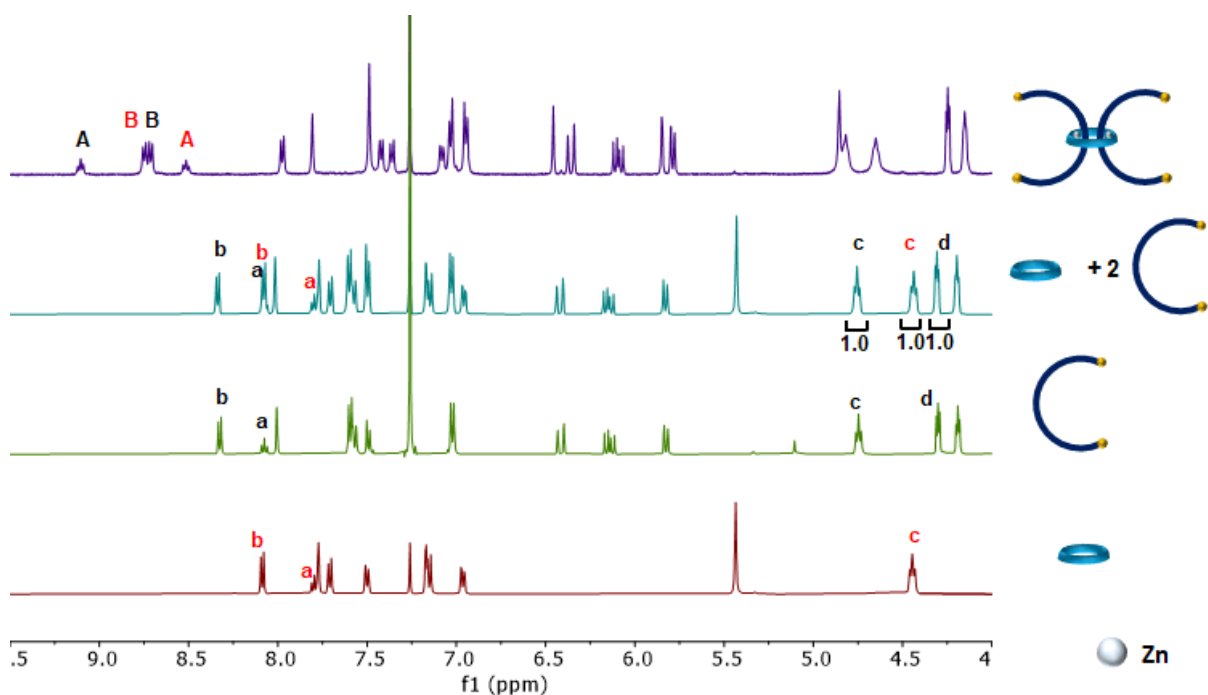


Figure S12. Partial ¹H NMR overlay (500 MHz, 25°C) of macrocycle **2⁴⁶**, thread **1**, the mixture of one **2⁴⁶** and two **1**, and **2⁴⁶** based P3R crosslinker (**1₂:2⁴⁶:Zn(II)₂**). ¹H assignments from Figure S11.

Synthesis of doubly threaded P3R crosslinker using **1**, **2**⁶⁸, and Zn(II)

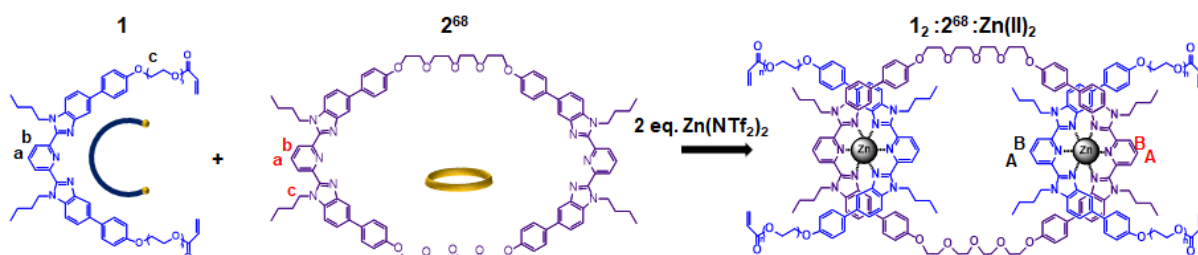


Figure S13. Synthesis of **2**⁶⁸ based P3R crosslinker (**1**₂:**2**⁶⁸:Zn(II)₂).

A solution of macrocycle **2**⁶⁸ (0.0108g, 0.007 mmol) was prepared using 1.0 mL of CDCl₃, and a solution of thread **1** (0.021g, 0.014 mmol) was prepared using 0.5 mL of CDCl₃. While monitoring both N-CH₂ peaks on the alkyl groups of the Bip ligands, the thread solution was titrated into the macrocycle solution until a precise 2:1 ratio was achieved. A solution of Zn(NTf₂)₂ was prepared with a concentration of 20 mM using a mixture of CDCl₃ and d₃-MeCN. The Zn(NTf₂)₂ solution was added until all unbound free Bip peaks (a, b) around 8.03 and 8.31 ppm disappeared. In the NMR spectrum of the resulting P3R crosslinkers, the new peaks (A, B) around 8.82 and 9.19 ppm appeared, indicating that all Bip ligands are bound with Zn²⁺ ions in a 2:1 ratio.

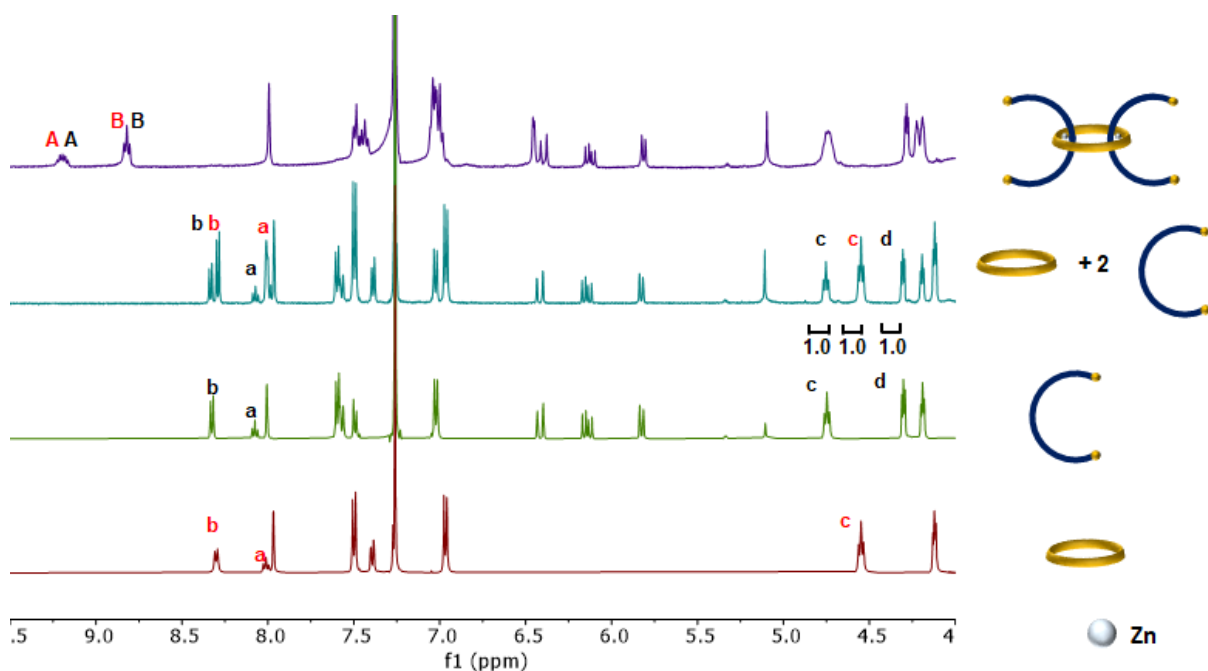


Figure S14. Partial ¹H NMR overlay (500 MHz, 25°C) of macrocycle **2**⁶⁸, thread **1**, the mixture of one **2**⁶⁸ and two **1**, and **2**⁶⁸ based P3R crosslinker (**1**₂:**2**⁶⁸:Zn(II)₂). ¹H assignments from Figure S13.

Synthesis of 4-arm supramolecular crosslinker using **1** and Zn(II)

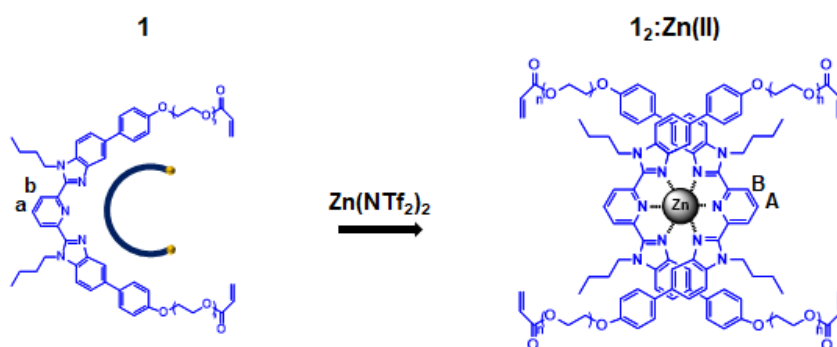


Figure S15. Synthesis of 4-arm supramolecular crosslinker (**12:Zn(II)**).

A solution of thread **1** (0.021g, 0.014 mmol) was prepared using 0.5 mL of CDCl₃. A solution of Zn(NTf₂)₂ was prepared with a concentration of 20 mM using a mixture of CDCl₃ and d₃-MeCN. The Zn(NTf₂)₂ solution was added until all unbound free Bip peaks (a, b) around 8.03 and 8.31 ppm disappeared. In the NMR spectrum of the resulting P3R crosslinkers, the new peaks (A, B) around 8.82 and 9.19 ppm appeared, indicating that all Bip ligands are bound with Zn²⁺ ions in a 2:1 ratio.

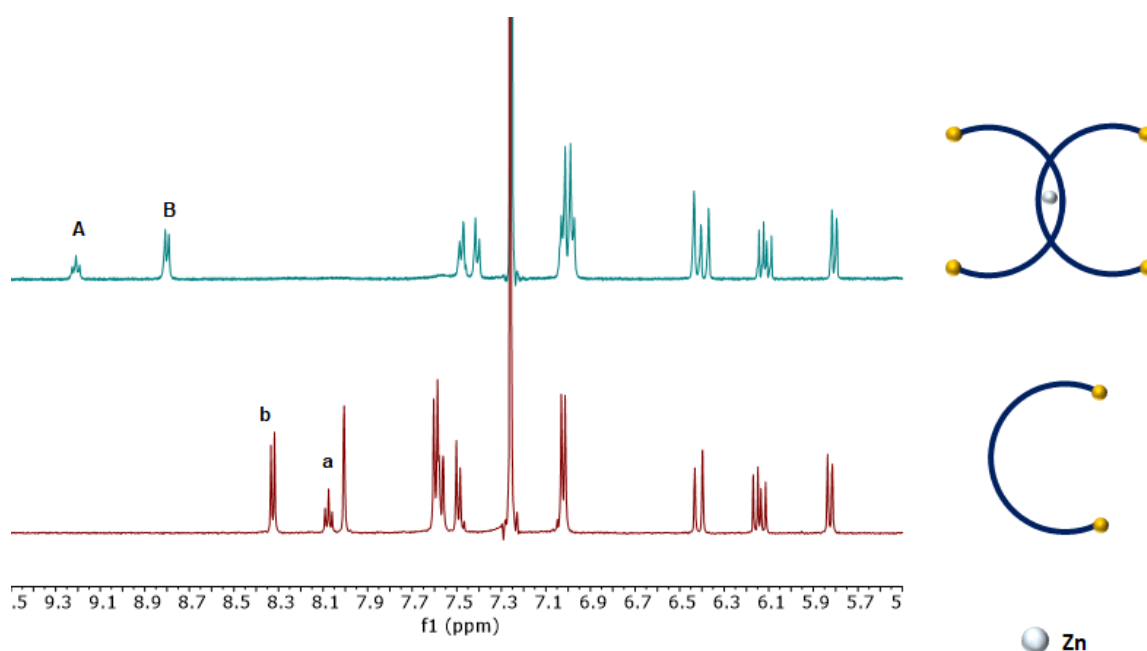


Figure S16. Partial ¹H NMR overlay (500 MHz, 25°C) of thread **1** and 4-arm supramolecular crosslinker (**12:Zn(II)**). ¹H assignments from Figure S15.

Fabrication of doubly threaded slide-ring gel networks (dt-SRGs), entangled gel network (EG), and covalent gel network (CG)

Gel networks	poly (ethylene glycol) methyl ether acrylate (PEG-MA), MW480	P3R crosslinker ($1_2:2^{56}:\text{Zn(II)}_2$) MW 4566	4-arm supramolecular crosslinker ($1_2:\text{Zn(II)}$) MW 3145	4-arm PEG acrylate MW 2000
dt-SRG $3^{56}_{1/99}$ (1 mol% P3R)	0.11088 mmol	0.00112 mmol	0	0
dt-SRG $3^{56}_{2/98}$ (2 mol% P3R)	0.05488 mmol	0.00112 mmol	0	0
dt-SRG $3^{56}_{3/97}$ (3 mol% P3R)	0.03621 mmol	0.00112 mmol	0	0
dt-SRG $3^{56}_{4/96}$ (4 mol% P3R)	0.02688 mmol	0.00112 mmol	0	0
EG $4_{3/97}$	0.03621 mmol	0	0.00112 mmol	0
CG $5_{3/97}$	0.03621 mmol	0	0	0.00112 mmol

Table S1. Composition of pre-gel solution for dt-SRGs $3^{56}_{X/Y}$, EG $4_{3/97}$, and CG $5_{3/97}$.

To prepare the pre-gel solution, solid crosslinkers were dissolved in liquid PEG-MA resin containing 0.5wt% of a photo-initiator (phenylbis(2,4,6-trimethylbenzoyl)phosphine oxide, BAPO) following the compositions listed in Table S1. The choice of crosslinker determined the type of gel network formed: P3R ($1_2:2^{56}:\text{Zn(II)}_2$) for dt-SRGs $3^{56}_{X/Y}$, the 4-arm supramolecular crosslinker ($1_2:\text{Zn(II)}$) for EG $4_{3/97}$, and a 4-arm PEG crosslinker for CG $5_{3/97}$. The pre-gel solutions were dropped onto a 1H,1H,2H,2H-perfluoro octyl trichlorosilane (PFOTS) coated glass slide^[7] with a spacer thickness of 450 μm , and they were covered with another PTFOTS-coated glass slide. Subsequently, these solutions were irradiated with long-wavelength ultraviolet light (Wavelength: 390-500 nm, Intensity: 200mW/cm²) using a filtered light source (Bluepoint 4 Ecocure from Honle UV America) for a total of 90minutes, consisting of 45minutes of upward irradiation followed by 45minutes of downward irradiation. The UV irradiation of the pre-gel solution initiated free-radical acrylic polymerization, generating the crosslinked networks (metalated dt-SRGs $3^{56}_{X/YM}$, metalated EG $4_{3/97M}$, and CG $5_{3/97}$).

To remove the uncrosslinked fraction, a chloroform washing step was conducted. The resulting gels were immersed in a large beaker containing 100mL of chloroform at 50°C on a hot plate. A cover glass was placed on top of the beaker, and the gels were iteratively washed with 100mL of chloroform and heated for 20 hours to extract the uncrosslinked fraction, which would be utilized for ring content calculation in the next section. After drying the gels under vacuum, metalated dt-SRGs $3^{56}_{X/YM}$, metalated EG $4_{3/97M}$, and CG $5_{3/97}$ were obtained.

For dt-SRGs 3^{56}_{XY} and EG $4_{3/97}$, further demetallation steps were conducted with tetrabutylammonium (TBAOH) to remove Zn^{2+} . The metalated gels (3^{56}_{XYM} or $4_{3/97M}$) were immersed in 30 mL of chloroform and 6 mL of methanol in a Teflon dish. Then, 10 μ L of a TBAOH solution (1M in methanol) was added to the dish and stirred for 30 minutes. The gels exhibited color and fluorescence changes, attributed to the decomplexation of zinc from the ligand. To extract metal salts and soluble fractions, iterative chloroform/methanol washing steps were conducted five times. Subsequently, the resulting gels were immersed in a large beaker containing 100mL of chloroform at 50°C on a hot plate for 20 hours to extract the soluble fractions, which would be utilized for ring content calculation in the next section. After drying the gels under vacuum, demetalated dt-SRGs 3^{56}_{XYD} and demetalated EG $4_{3/97}$ were obtained. The gel fraction (GF) was calculated using the following Equation S1:

$$GF \text{ (wt\%)} = \frac{W_{dry, after chloroform washing and demetalation}}{W_{dry, crude, take into account the metal ion salt}} \times 100 \quad (S1)$$

Where $W_{dry, after chloroform washing and demetalation}$ represents the weight of the dried gel after chloroform washing and demetalation, and $W_{dry, crude}$ represents the weight of the dried gel after photocrosslinking. $W_{dry, crude, take into account the metal ion salt}$ was adjusted to take into account the presence of metal ion salt. For CG without demetallation step, GF was calculated by using $W_{dry, after chloroform washing}$ and $W_{dry, crude}$ without taking in account the presence of metal ion salt.

Additionally, a remetallation step was conducted with $Zn(NTf_2)_2$. The demetalated gels were immersed in 30 mL of chloroform and 6 mL of methanol in a Teflon dish. 0.00224 mmol of $Zn(NTf_2)_2$ solution in 5mL of acetonitrile was added to the dish and stirred for 3 hours. Similar to the demetallation process, the gels exhibited color and fluorescence changes attributed to the re-complexation of ligand and zinc.

Characterization of dt-SRGs, EG, and CG

UV-Vis absorbance and fluorescence spectra of dt-SRG upon demetalation

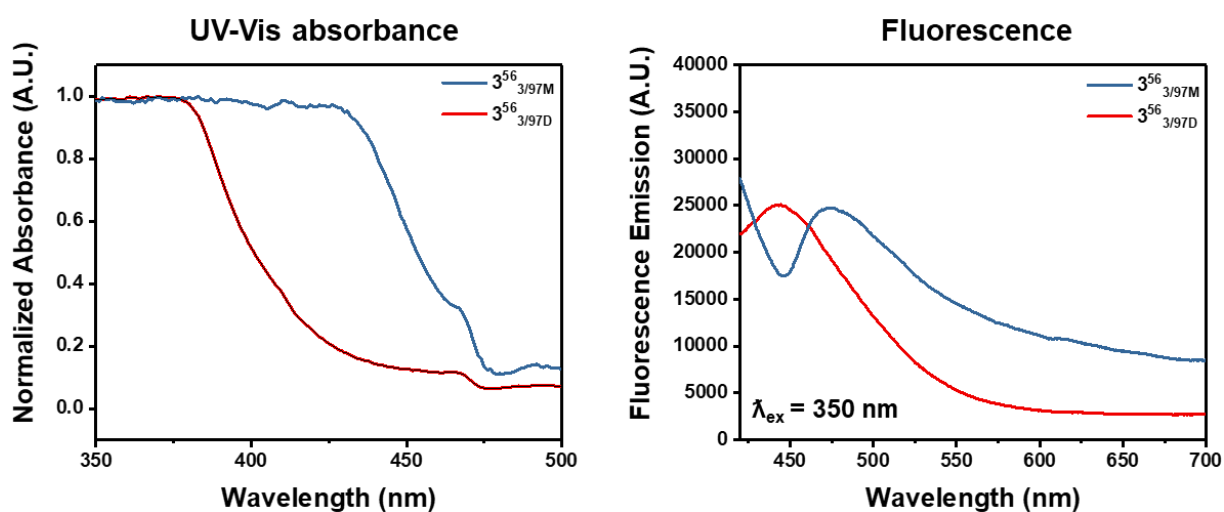


Figure S17. UV-Vis (left) and fluorescence (right, excitation wavelength: 350nm) spectra of the metalated dt-SRG $3^{56}_{3/97M}$ and the demetalated dt-SRG $3^{56}_{3/97D}$. Gels were fully swollen in propylene carbonate (PC). Swollen gel was cut into circular ($D = 10\text{mm}$) and placed onto a quartz glass slide.

FT-IR spectra of dt-SRG

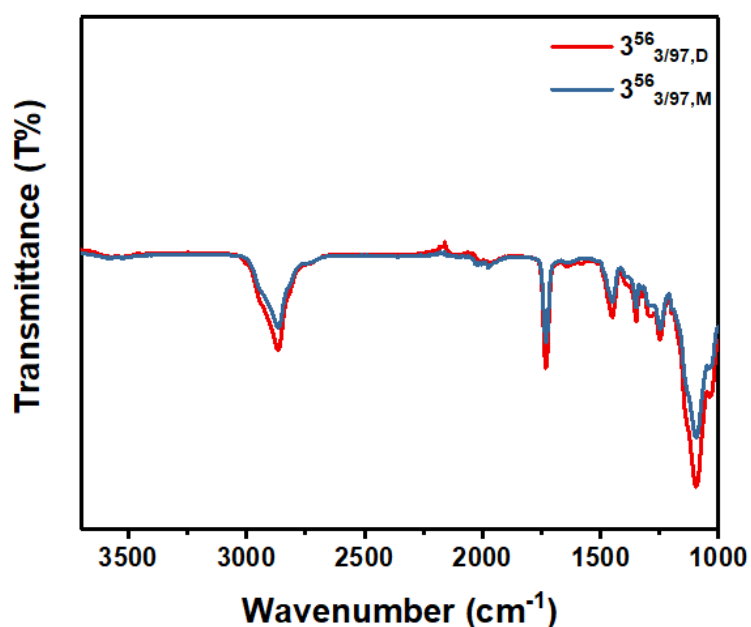


Figure S18. FT-IR spectra of the metalated dt-SRG $3^{56}_{3/97M}$ and demetalated dt-SRG $3^{56}_{3/97D}$.

NMR study for the calculation of ring content within dt-SRGs

For dt-SRGs, it is crucial to calculate the ring content of the gels, indicating how many macrocycles remain within the gel networks after (1) the chloroform washing step (metalated soluble fraction) and (2) the demetalation step (demetalated soluble fraction). With the external standard NMR method, the ring content was determined by comparing the molar ratio of a reference molecule (thymol) to the macrocycle (MC) in the metalated soluble fraction and demetalated soluble fraction. To quantify the mole number of macrocycles in the metalated soluble fraction, the soluble fraction was demetalated and purified by the following steps. The soluble fractions were dissolved in 5 mL of DCM with the subsequent addition of 5 μ L of TBAOH solution (1M in MeOH). Each soluble fraction was then washed with 15 mL of DI water and then the organic layer was subsequently dried under vacuum. The resulting soluble fractions were dissolved in 500 μ L of CDCl_3 and then transferred to each NMR tube. For external standard, the thymol standard (NMR *TraceCERT*[®], 0.00050 g) was also dissolved in 100 μ L of CDCl_3 and then transferred to Wilmad[®] coaxial insert tube. The same coaxial insert tube was added to each NMR tube containing the metalated or demetalated soluble fractions.

The relationship between the number (moles) of MC in the soluble fraction and the reference thymol is determined by the integral of the diagnostic proton peak and the number of protons contributing to the peak using the following Equation S2:

$$X_{MC,Sol} = \frac{I_{MC}}{I_{Std}} \times \frac{N_{Std}}{N_{MC}} \times X_{Std} \quad (\text{S2})$$

where X_{MC} represents the number of moles of macrocycles in the soluble fraction, X_{Std} represents the number of moles of thymol (known), I_{MC} or I_{Std} represents the integrated area of the diagnostic proton peak, and N_{MC} or N_{Std} represents the number of protons contributing to the peak. X_{Std} , N_{MC} , and N_{Std} are known values, and I_{MC} and I_{Std} are measured via ^1H NMR.

The G peak (N=8) of the macrocycle at 6.85 ppm was compared to the A peak (N=1) of the thymol standard at 6.73 ppm, resulting in the calculation of $X_{MC, sol}$ (**Fig. S19**). Additionally, ^1H T1 measurements were conducted for the G peak of the macrocycle and the A peak of the thymol standard before comparing the integral of these two peaks (**Fig. S20**). These experiments were conducted using the standard Bruker inversion-recovery experiment “t1ir” with a relaxation delay $D1 = 15$ seconds and 10 interpulse recovery delays ranging from 0.01 to 15.0 seconds following the Bruker Advanced NMR Methods manual^[8]. T1 values were obtained by fitting data to a recovery function using Bruker Topspin software. The T1 value of

the A peak and G peak was observed to be lower than $\frac{D1}{3}$. Consequently, the integral of these peaks could be reliably compared with an accuracy exceeding 95%. As shown in **Figure S19**, the G peak of macrocycles was observed in the demetalated soluble fraction, indicating that a small number of macrocycles were dethreaded during only the demetalation step. The average mole number of macrocycle present in each soluble fraction of dt-SRGs is listed in Table S2. With $X_{MC, Sol}$ values, both $X_{MC, Gel}$ and ring content are calculated by using Equations S3 and S4.

$$X_{MC, Gel} = X_{MC, added} - X_{MC, Sol} \quad (S3)$$

$$Ring\ content\ (\%) = \frac{X_{MC, Gel}}{X_{MC, added}} \times 100 \quad (S4)$$

where $X_{MC, added}$ represents the number of moles of MC in pre-gel solution.

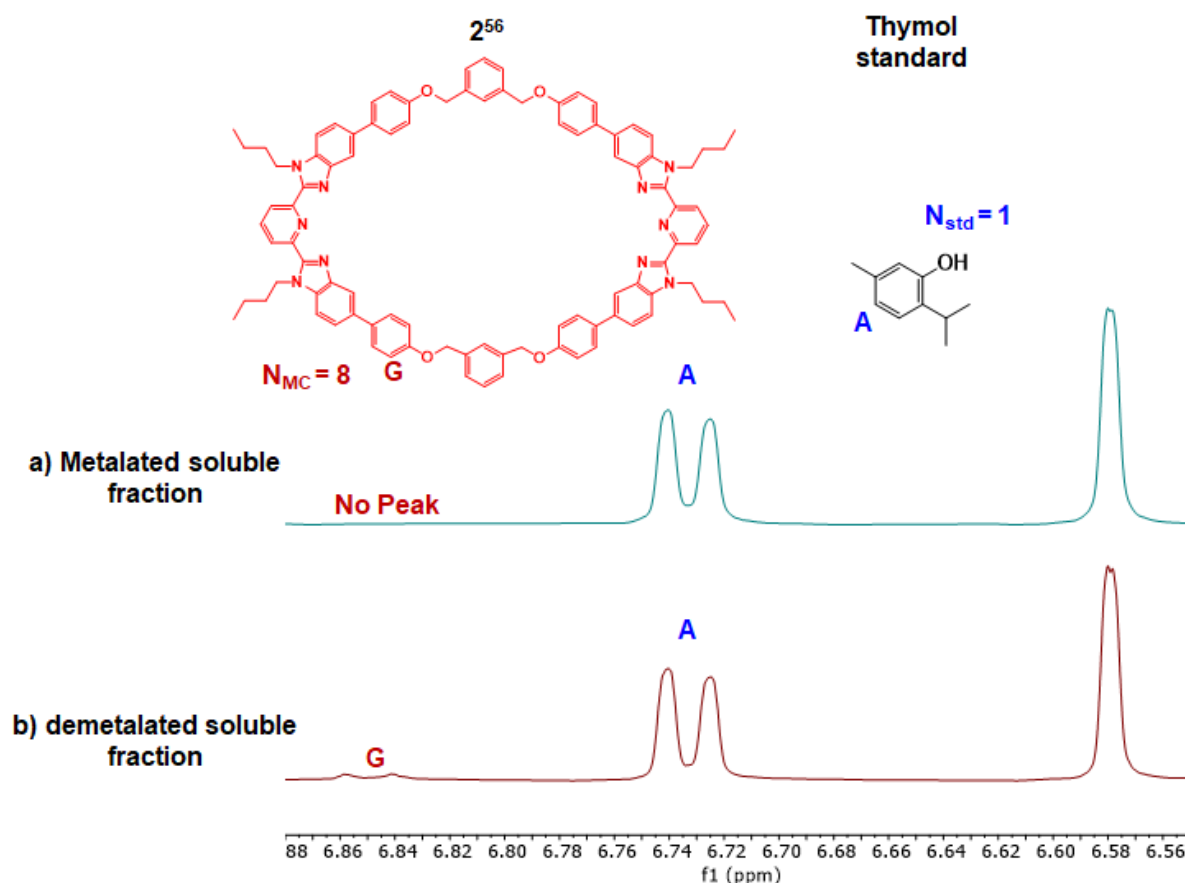


Figure S19. Partial 1H NMR overlay (500 MHz, 25°C, $CDCl_3$) of (a) the metalated soluble fractions and (b) the demetalated soluble fractions of dt-SRG $3^{56}_{3/97}$ containing thymol as an external NMR standard. The integrals of the doublet at 6.85 ppm (G, red) for 2^{56} MC ($N=8$), I_{MC} , and the doublet at 6.73 ppm (A, blue) for thymol ($N=1$), I_{Std} , were used to calculate the moles of macrocycle 2^{56} (X_{MC}) in each soluble fraction. All spectra were referenced to the thymol singlet at 6.58 ppm. Full 1H NMR assignments for 2^{56} from Figure S5.

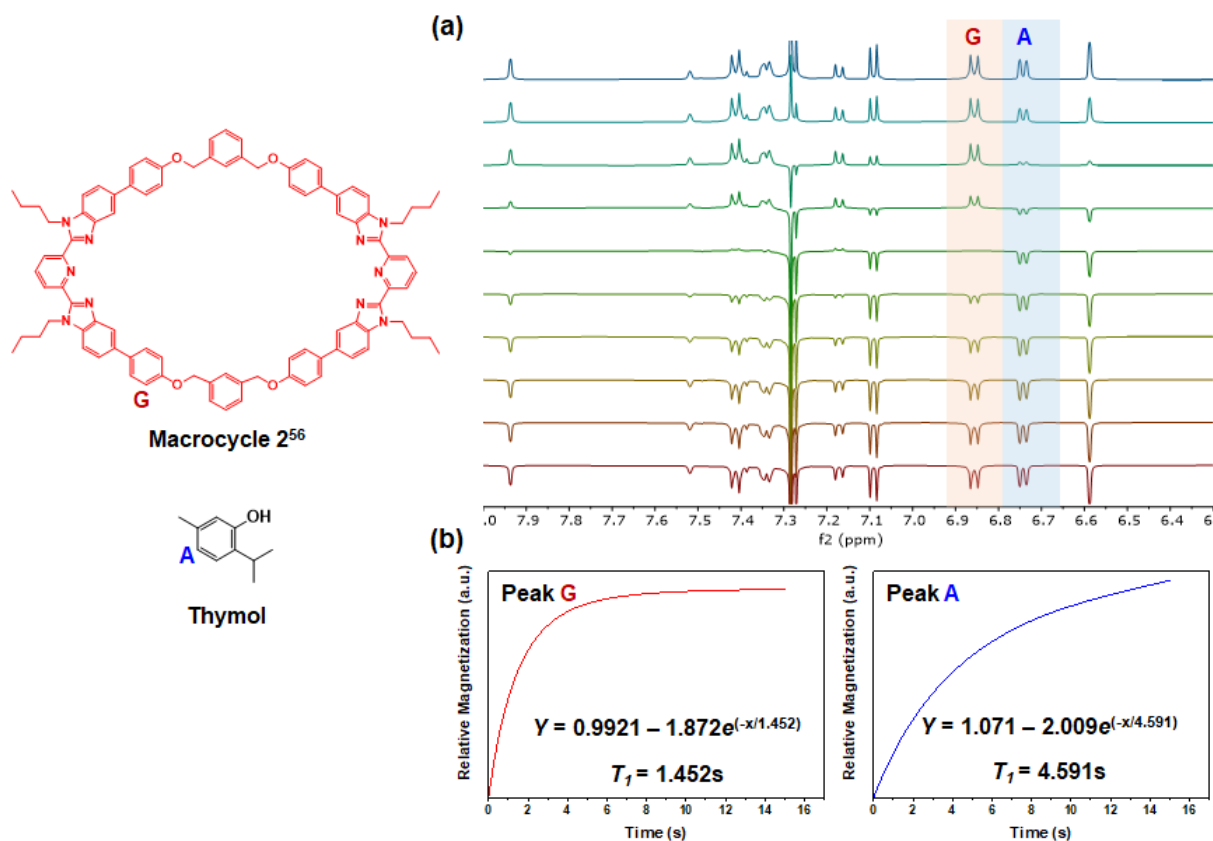


Figure S20. (a) Partial ^1H NMR stack of relaxation measurement on 2^{56} with thymol reference showing 10 different spectra with varying inversion recovery delays (longest at the top). (b) Plot showing relative magnetization versus time calculated from the three-parameter exponential fit ($I_0 + P \cdot \exp(-t/T_1)$) for peak G (red) and peak A (blue).

Gel networks	$X_{MC, added}$ (mmol)	$I_{MC, Met, Sol}$	$I_{MC, Met, Sol}$	I_{Thymol}	$X_{MC, Sol}$ (mmol)	$X_{MC, Gel}$ (mmol)	X_{Thymol} (mmol)
dt-SRG $3^{56}_{1/99}$ (1 mol% P3R)	0.00112	0	10	100	0.000041625	0.00107837	0.00333
dt-SRG $3^{56}_{2/98}$ (2 mol% P3R)	0.00112	0	7.3	100	0.000030386	0.00108961	0.00333
dt-SRG $3^{56}_{3/97}$ (3 mol% P3R)	0.00112	0	6.7	100	0.000027888	0.00109211	0.00333
dt-SRG $3^{56}_{4/96}$ (4 mol% P3R)	0.00112	0	8.5	100	0.000035381	0.00108461	0.00333

Table S2. The average mole number of macrocycle present in each soluble fraction of dt-SRGs, thymol, and pre-gel solution.

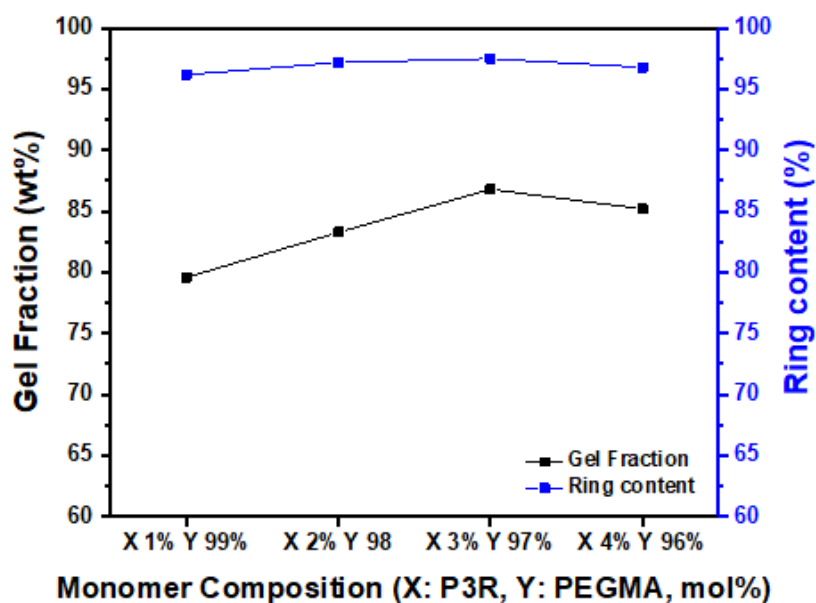


Figure S21. Gel fraction and ring content of demetalated dt-SRGs $3^{56}_{X/YD}$ (X represents mol% of P3R crosslinker $1_2:2^{56}:\text{Zn(II)}_2$ and Y represents mol% of PEGMA, $Y=100-X$).

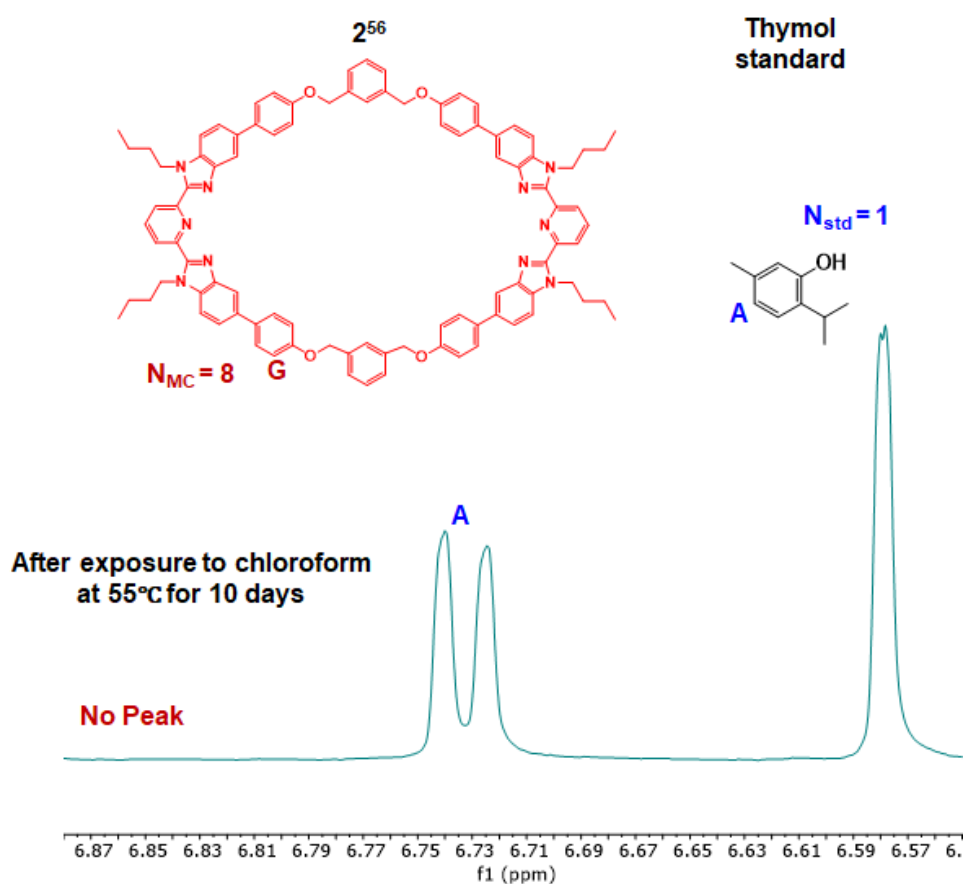


Figure S22. ^1H NMR overlay (500 MHz, 25°C , CDCl_3) of the washed solution in dt-SRG $3^{56}_{3/97D}$ containing thymol as an external NMR standard. dt-SRG $3^{56}_{3/97D}$ were exposed to chloroform at 50°C for 10 days, and the washed chloroform solution was collected to confirm that macrocycles did not dethread at high temperature. Full ^1H NMR assignments for 2^{56} from Figure S5.

Gel fraction of dt-SRG $3^{56}_{3/97}$, EG $4_{3/97}$, and CG $5_{3/97}$

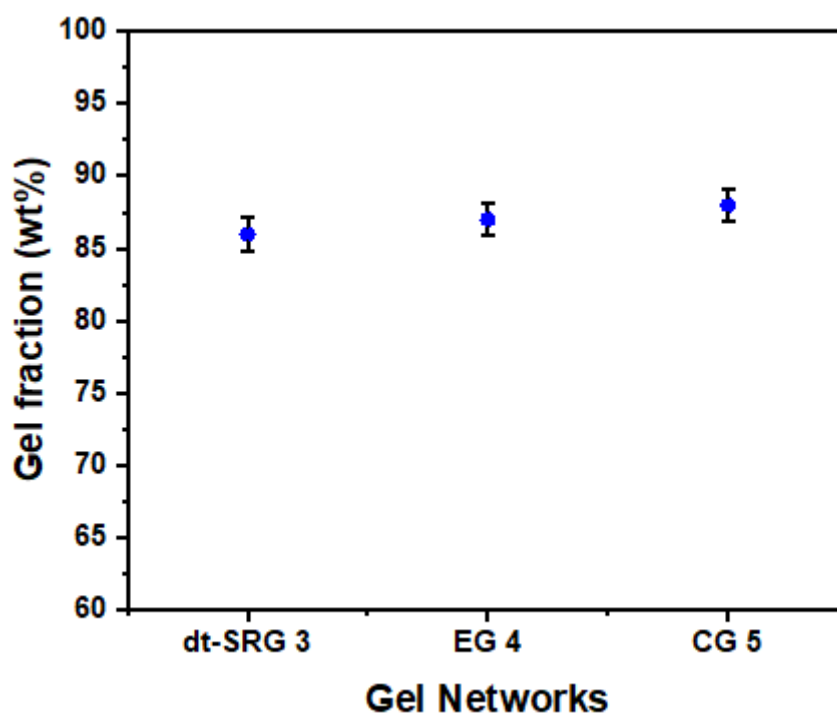


Figure S23. Gel fraction of dt-SRG $3^{56}_{3/97}$, EG $4_{3/97}$, and CG $5_{3/97}$. These gel networks are crosslinked by polymerizing 97mol% of PEG-MA with 3mol% of crosslinkers ($1_2:2^{56}:\text{Zn(II)}_2$ for dt-SRG $3^{56}_{3/97}$, $1_2:\text{Zn(II)}$ for EG $4_{3/97}$, and a 4-arm PEG crosslinker for CG $5_{3/97}$). Monomer compositions are listed in Table. S1.

Differential scanning calorimetry (DSC) measurement

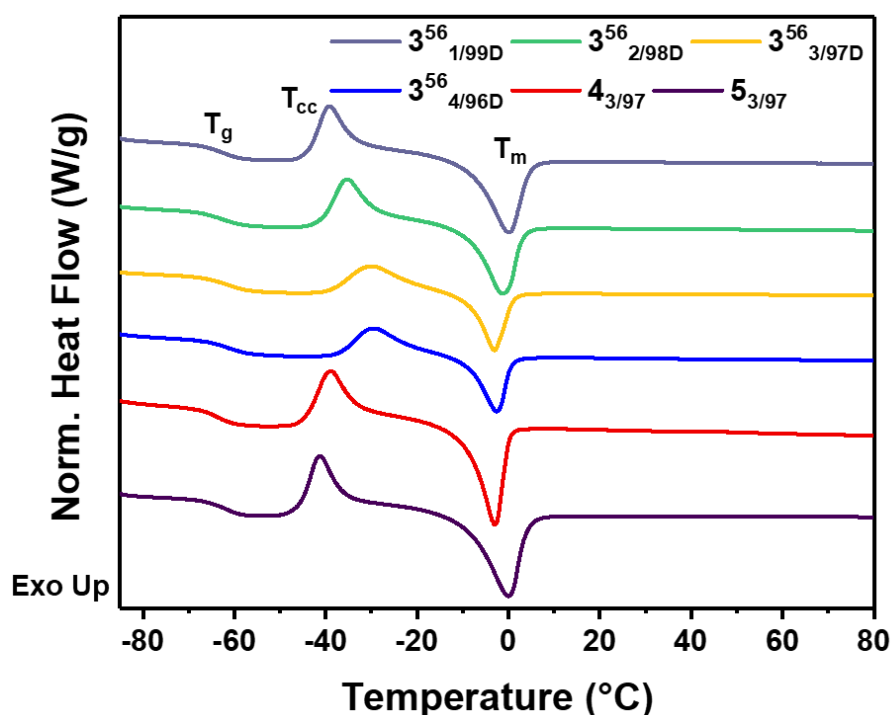


Figure S24. Differential scanning calorimetry (DSC) curves of the film of dt-SRGs $3^{56}_{X/YD}$ (X represents mol% of P3R crosslinker $1_2:2^{56}:\text{Zn(II)}_2$ and Y represents mol% of PEGMA, Y=100-X), and EG $4_{3/97}$ and CG $5_{3/97}$ during second heating (Exotherm up, ramp rate = $10^\circ\text{C}/\text{min}$). $4_{3/97}$ was prepared by copolymerizing 3mol% of 4-arm supramolecular crosslinker ($1_2:\text{Zn(II)}$) with 97mol% of PEG-MA, and $5_{3/97}$ was prepared by copolymerizing 3mol% of 4-arm PEG crosslinker (Monomer compositions are listed in Table. S1).

Gel networks	T_g ($^\circ\text{C}$)	T_{cc} ($^\circ\text{C}$)	T_m ($^\circ\text{C}$)
dt-SRG $3^{56}_{1/99D}$ (1 mol% P3R)	-63.11	-39.12	-0.10
dt-SRG $3^{56}_{2/98D}$ (2 mol% P3R)	-62.89	-35.22	-1.30
dt-SRG $3^{56}_{3/97D}$ (3 mol% P3R)	-61.70	-29.74	-3.19
dt-SRG $3^{56}_{4/96D}$ (4 mol% P3R)	-61.34	-29.38	-2.65
EG $4_{3/97}$	-64.67	-39.42	-3.33
CG $5_{3/97}$	-62.72	-41.27	-0.30

Table S3. Thermal properties of the film of dt-SRGs $3^{56}_{X/YD}$ (X=mol% of P3R and Y=mol% of PEGMA), EG $4_{3/97}$, and CG $5_{3/97}$.

UV-Vis absorbance and fluorescence spectra of dt-SRG upon remetallation

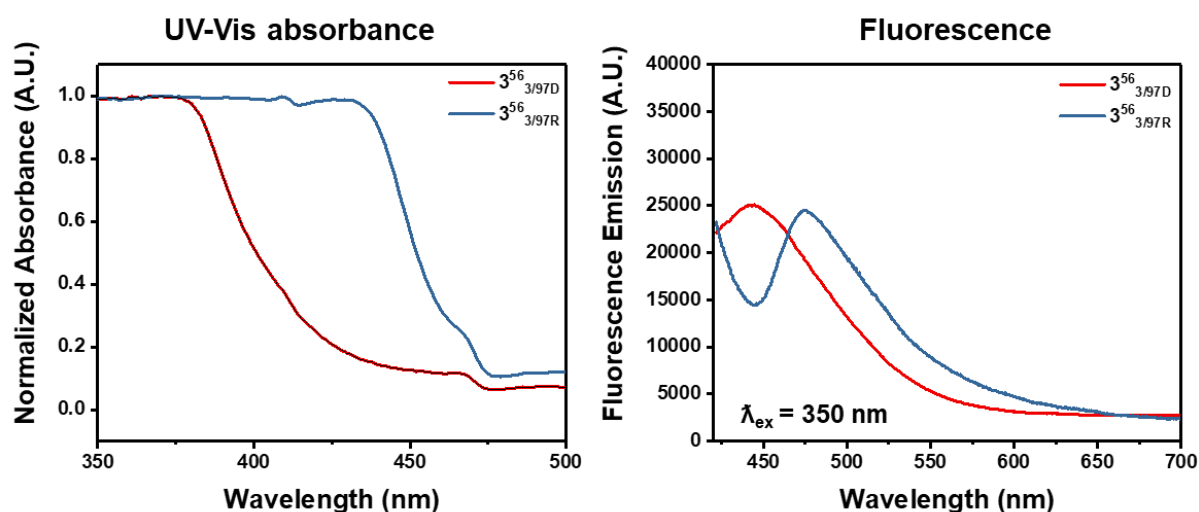


Figure S25. UV-Vis (left) and fluorescence (right, excitation wavelength: 350nm) spectra of the demetalated dt-SRG $3^{56}_{3/97D}$ and the remetalled dt-SRG $3^{56}_{3/97R}$. Gels were fully swollen in propylene carbonate (PC). Swollen gel was cut into circular ($D = 10\text{mm}$) and placed onto a quartz glass slide.

Swelling behavior of dt-SRG $3^{56}_{3/97}$, EG $4_{3/97}$, and CG $5_{3/97}$

A sieve filtration method was utilized to ensure repeatable and reproducible measurement of the swelling ratio. This method involved completely removing excess fluid from the gel on a wire mesh sieve using vacuum filtration^[9]. The mass of a 316 stainless steel wire sieve (250 x 250 mesh size, 0.0024" opening size) was recorded as W_1 . The gels were placed in a vacuum oven overnight at approximately 25°C, and their mass in a dry state was recorded as W_0 . The gels were then immersed in 50 mL of solvent for 24 hours at room temperature to allow the gels to reach their swelling equilibrium. Once fully swollen, the gels were poured onto the wire sieve under a vacuum to remove excess solvent from the gel (and sieve), and the mass of the sieve with the gel on it was recorded as W_2 . The swelling ratio was calculated by following Equation S5:

$$\text{Swelling Ratio (wt\%)} = \frac{W_2 - W_1 - W_0}{W_0} \quad (\text{S5})$$

Viscoelastic properties of dt-SRG $3^{56}_{3/97}$, EG $4_{3/97}$, and CG $5_{3/97}$

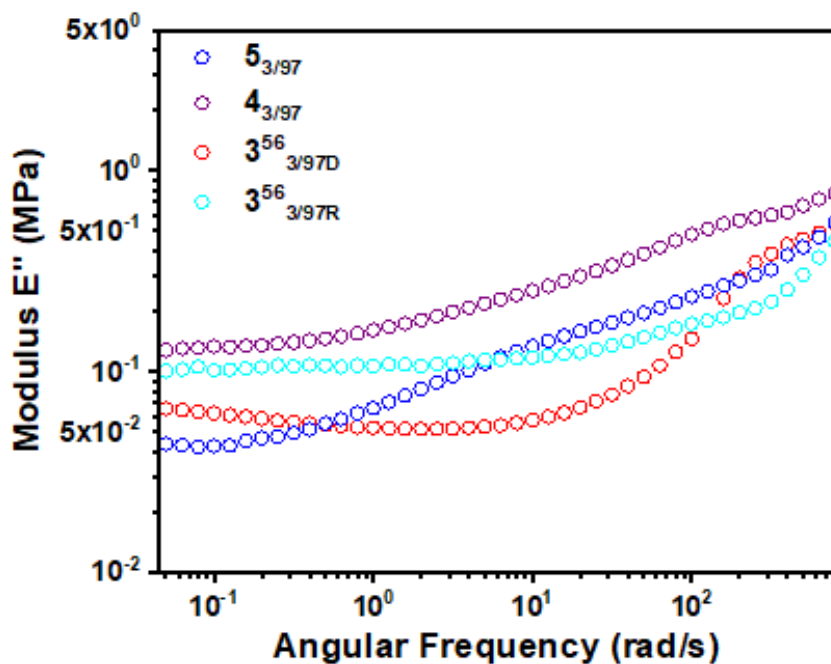


Figure S26. Loss moduli E'' of demetalated dt-SRG $3^{56}_{3/97D}$ (red), remetalated dt-SRG $3^{56}_{3/97R}$ (cyan), EG $4_{3/97}$ (purple), and CG $5_{3/97}$ (blue) fully swollen in PC.

Macroscopic stress relaxation properties of dt-SRG $3^{56}_{3/97}$, EG $4_{3/97}$, and CG $5_{3/97}$

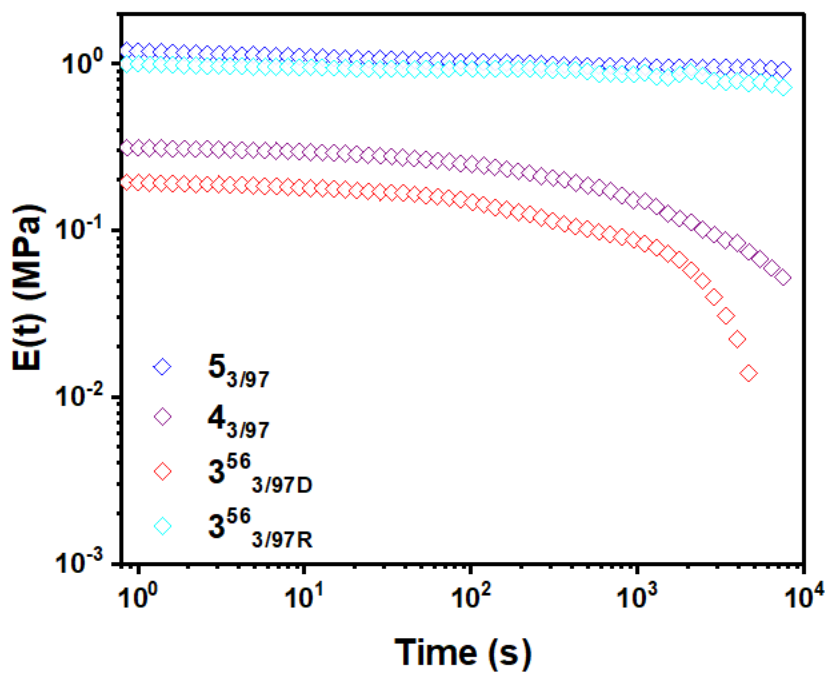


Figure S27. Relaxation moduli $E(t)$ of demetalated dt-SRG $3^{56}_{3/97D}$ (red), remetalated dt-SRG $3^{56}_{3/97R}$ (cyan), EG $4_{3/97}$ (purple), and CG $5_{3/97}$ (blue) fully swollen in PC.

Fabrication and characterization of dt-SRGs with different ring sizes

To prepare the pre-gel solution, solid P3R crosslinkers were dissolved in liquid PEG-MA resin containing 0.5wt% of a photo-initiator (BAPO) according to the compositions listed in Table S4. The choice of crosslinker determine the type of gel network formed: $1_2:2^{46}:\text{Zn(II)}_2$ for dt-SRG $3^{46}_{3/97}$, $1_2:2^{56}:\text{Zn(II)}_2$ for dt-SRG $3^{56}_{3/97}$, and $1_2:2^{68}:\text{Zn(II)}_2$ for dt-SRG $3^{68}_{3/97}$. The pre-gel solutions were dispensed onto a perfluoro octyl trichlorosilane (PFOTS) coated glass slide with a spacer thickness of 450 μm , and covered with another PTFOTS-coated glass slide. Subsequently, these solutions were irradiated with long-wavelength ultraviolet light (Wavelength: 390-500 nm, Intensity: 200mW/cm²) using a filtered light source (Bluepoint 4 Ecocure from Honle UV America) for a total of 90minutes, consisting 45minutes of upward irradiation followed by 45minutes of downward irradiation. The UV irradiation of the pre-gel solution initiated free-radical acrylic polymerization, generating the crosslinked gel networks.

To remove the uncrosslinked fraction, a chloroform washing step was conducted. The resulting gels were immersed in a large beaker containing 100mL of chloroform at 50°C on a hot plate. A cover glass was placed on top of the beaker, and the gels were iteratively washed with 100mL of chloroform and heated for 20 hours to extract the uncrosslinked fraction, which would be utilized for ring content calculation. After drying the gels under vacuum, metalated dt-SRGs ($3^{46}_{3/97\text{M}}$ and $3^{68}_{3/97\text{M}}$) were obtained. Next, demetalation steps were conducted with tetrabutylammonium (TBAOH) to remove Zn^{2+} . The metalated gels were immersed in 30 mL of chloroform and 6 mL of methanol in a Teflon dish. Then, 10 μL of TBAOH solution (1M in methanol) was added to the dish and stirred for 30 minutes. The gels exhibited color and fluorescence changes, attributed to the decomplexation of ligand and zinc. To extract metal salts and soluble fractions, iterative chloroform/methanol washing steps were conducted five times. Subsequently, the resulting gels were immersed in a large beaker containing 100mL of chloroform at 50°C on a hot plate for 20 hours to extract the soluble fractions, which would be utilized for ring content calculation. After drying the gels under vacuum, demetalated dt-SRGs ($3^{46}_{3/97\text{D}}$ and $3^{68}_{3/97\text{D}}$) were obtained. The gel fraction (GF) was calculated using Equation S1. Their ring contents were calculated using Equation S2-S4.

Gel networks	poly (ethylene glycol) methyl ether acrylate (PEG-MA) MW = 480	2^{46} based P3R crosslinker ($1_2:2^{46}:\text{Zn(II)}_2$)	2^{56} based P3R crosslinker ($1_2:2^{56}:\text{Zn(II)}_2$)	2^{68} based P3R crosslinker ($1_2:2^{68}:\text{Zn(II)}_2$)
dt-SRG $3^{46}_{3/97}$	0.03621 mmol	0.00112 mmol	0	0
dt-SRG $3^{56}_{3/97}$	0.03621 mmol	0	0.00112 mmol	0
dt-SRG $3^{68}_{3/97}$	0.03621 mmol	0	0	0.00112 mmol

Table S4. Composition of pre-gel solution for three dt-SRGs.

Gel fraction and ring content of dt-SRGs $3^{46}_{3/97D}$, $3^{56}_{3/97D}$, $3^{68}_{3/97D}$

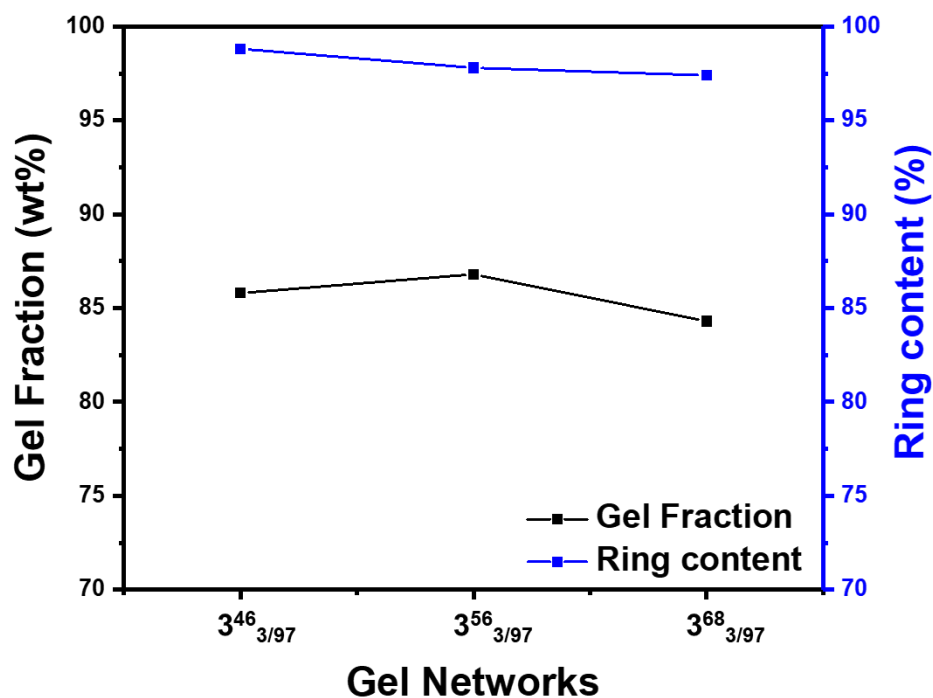


Figure S28. Gel fractions and ring content of three dt-SRGs ($3^{46}_{3/97D}$, $3^{56}_{3/97D}$, and $3^{68}_{3/97D}$).

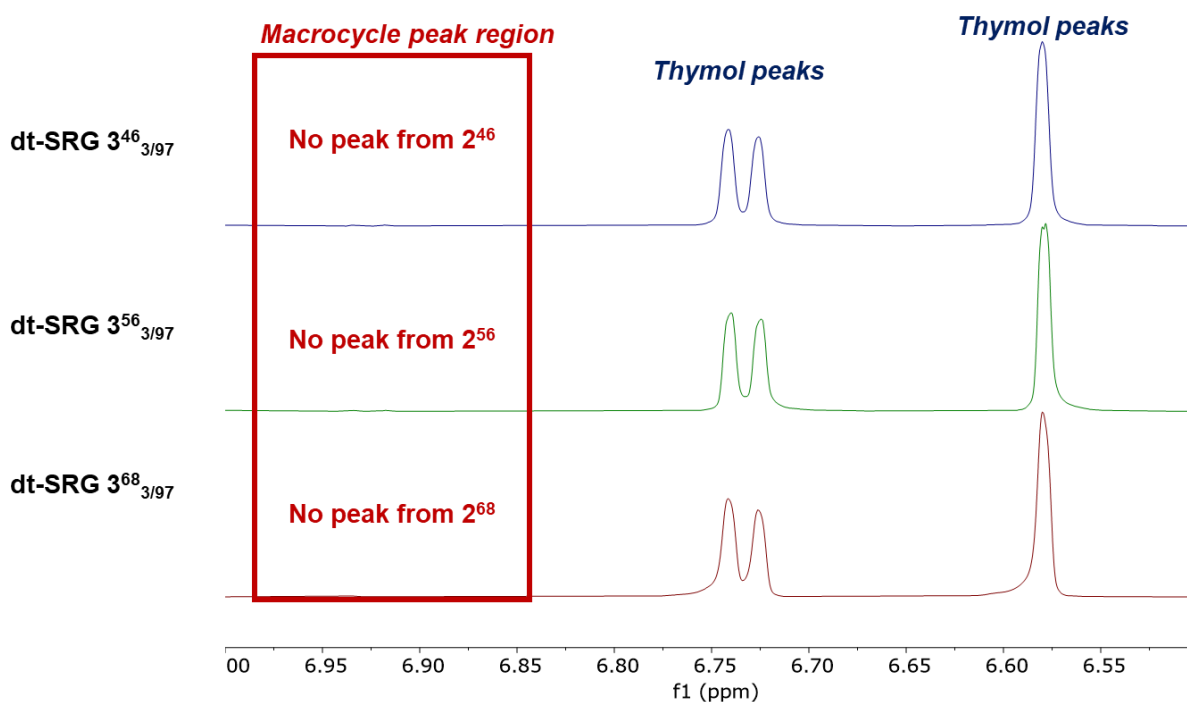


Figure S29. ^1H NMR overlay (500 MHz, 25°C , CDCl_3) of the washed solution in three dt-SRGs ($3^{46}_{3/97}$, $3^{56}_{3/97}$, and $3^{68}_{3/97}$) containing thymol as an external NMR standard. dt-SRGs ($3^{46}_{3/97}$, $3^{56}_{3/97}$, and $3^{68}_{3/97}$) were exposed to chloroform at 50°C for 10 days, and the washed chloroform solution was collected to confirm that macrocycles did not dethread at high temperature.

Swelling behaviors of dt-SRGs $3^{46}_{3/97D}$, $3^{56}_{3/97D}$, $3^{68}_{3/97D}$

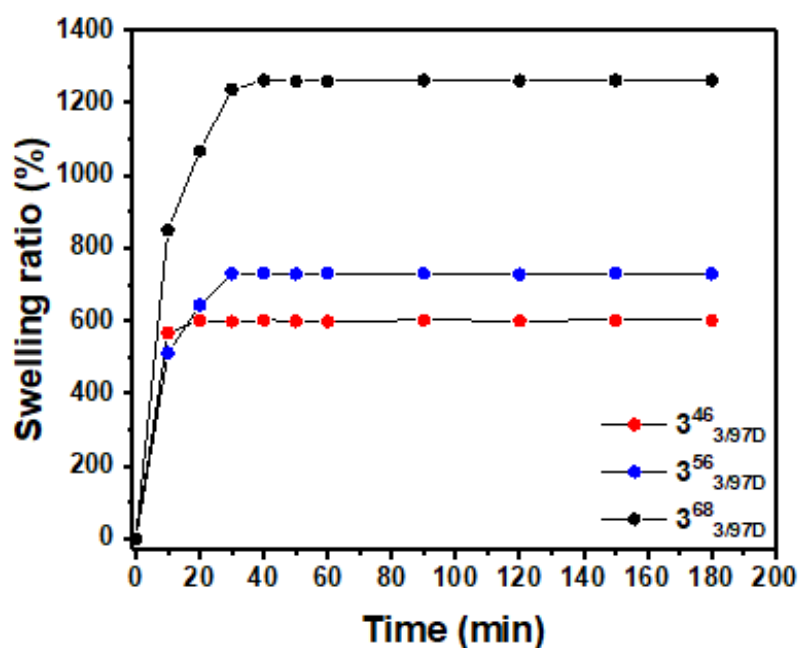


Figure S30. Graph of swelling ratio versus time for three demetalated dt-SRGs ($3^{46}_{3/97D}$, $3^{56}_{3/97D}$, and $3^{68}_{3/97D}$) upon exposure to propylene carbonate.

Viscoelastic properties of dt-SRGs $3^{46}_{3/97D}$, $3^{56}_{3/97D}$, $3^{68}_{3/97D}$

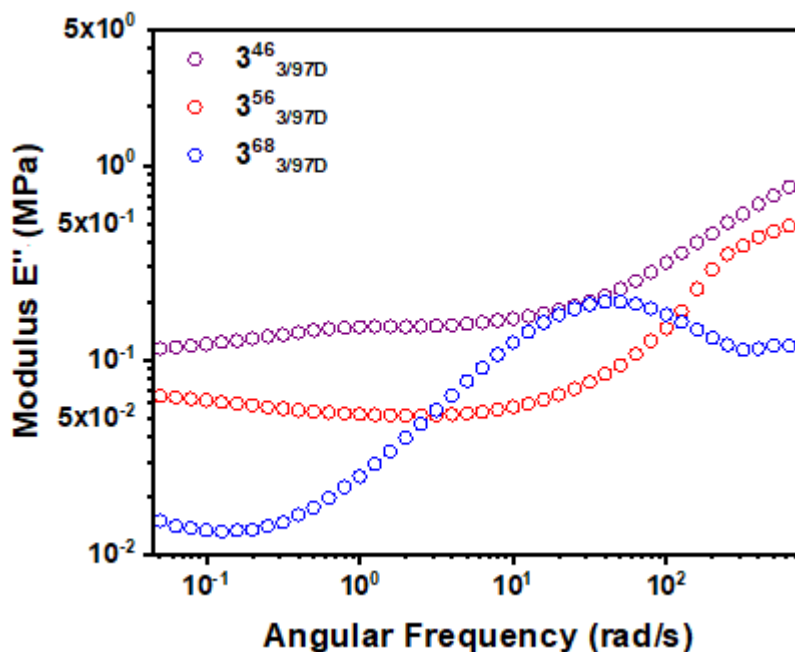


Figure S31. Loss moduli E'' of demetalated dt-SRGs $3^{46}_{3/97D}$ (purple), $3^{56}_{3/97D}$ (red), $3^{68}_{3/97D}$ (blue) fully swollen in PC.

Macroscopic stress relaxation properties of dt-SRGs $3^{46}_{3/97D}$, $3^{56}_{3/97D}$, $3^{68}_{3/97D}$

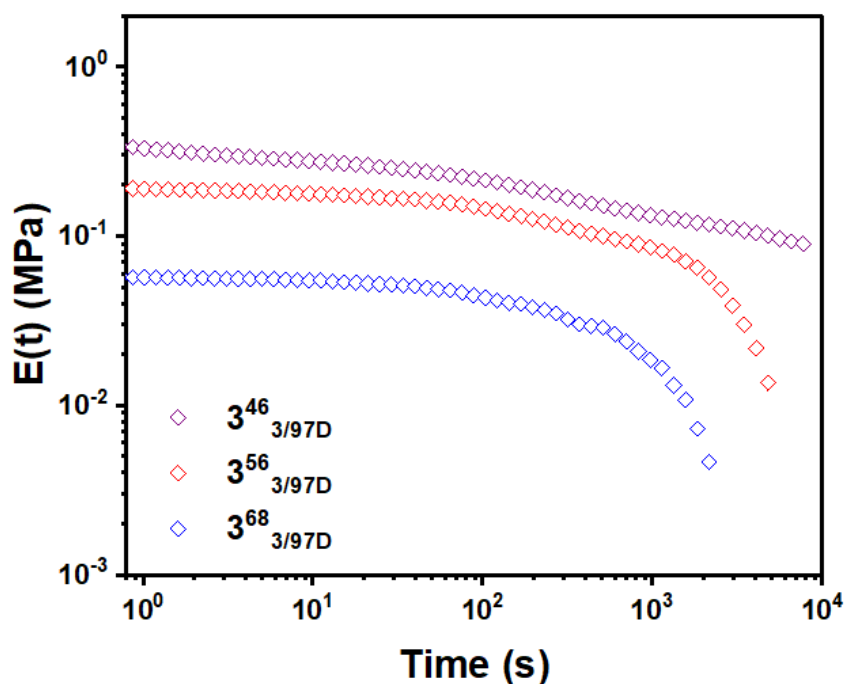


Figure S32. Relaxation moduli $E(t)$ of demetalated dt-SRGs $3^{46}_{3/97D}$ (purple), $3^{56}_{3/97D}$ (red), $3^{68}_{3/97D}$ (blue) fully swollen in PC.

DOSY spectra and diffusion coefficients of macrocycles

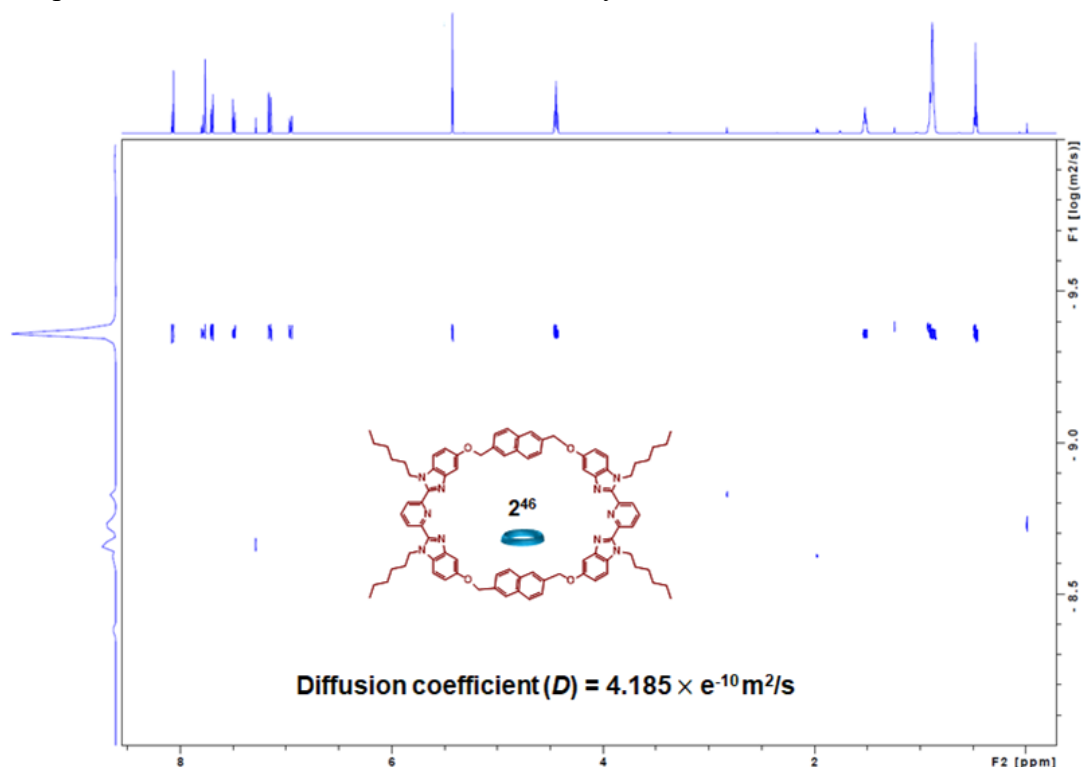


Figure S33. DOSY Spectrum (500 MHz, 25°C) and diffusion coefficient of 5mM of 2^{46} (Solvent: 5% acetonitrile- d_3 in chloroform- d).

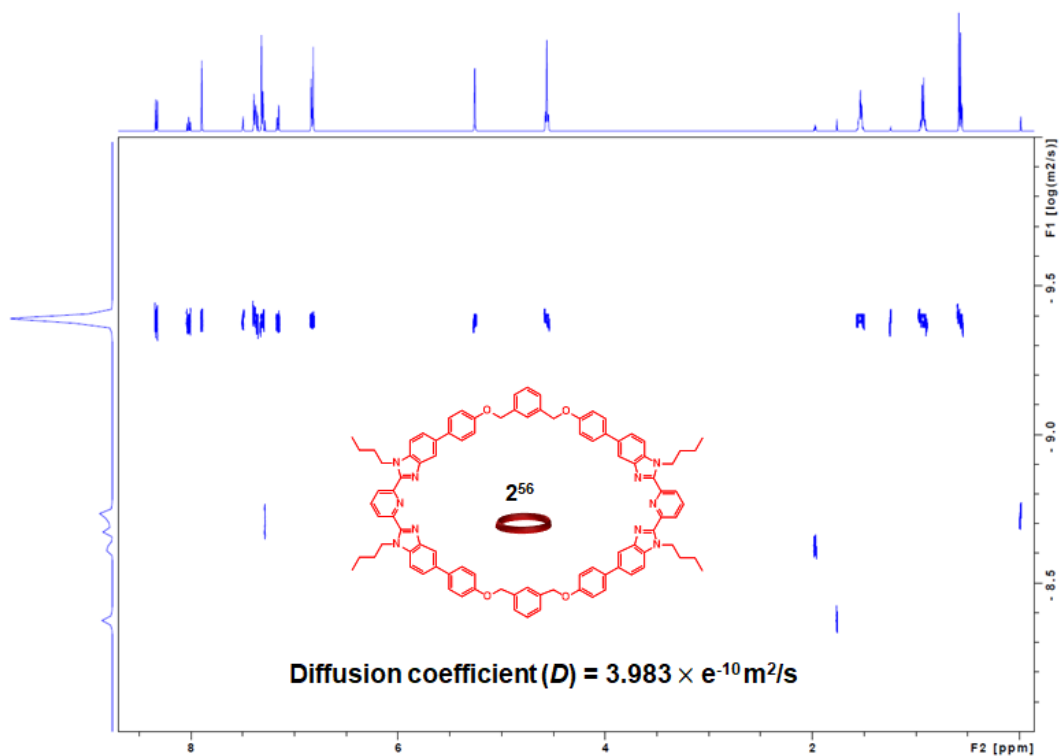


Figure S34. DOSY Spectrum (500 MHz, 25°C) and diffusion coefficient of 5mM of **2⁵⁶** (Solvent: 5% acetonitrile-*d*₃ in chloroform-*d*).

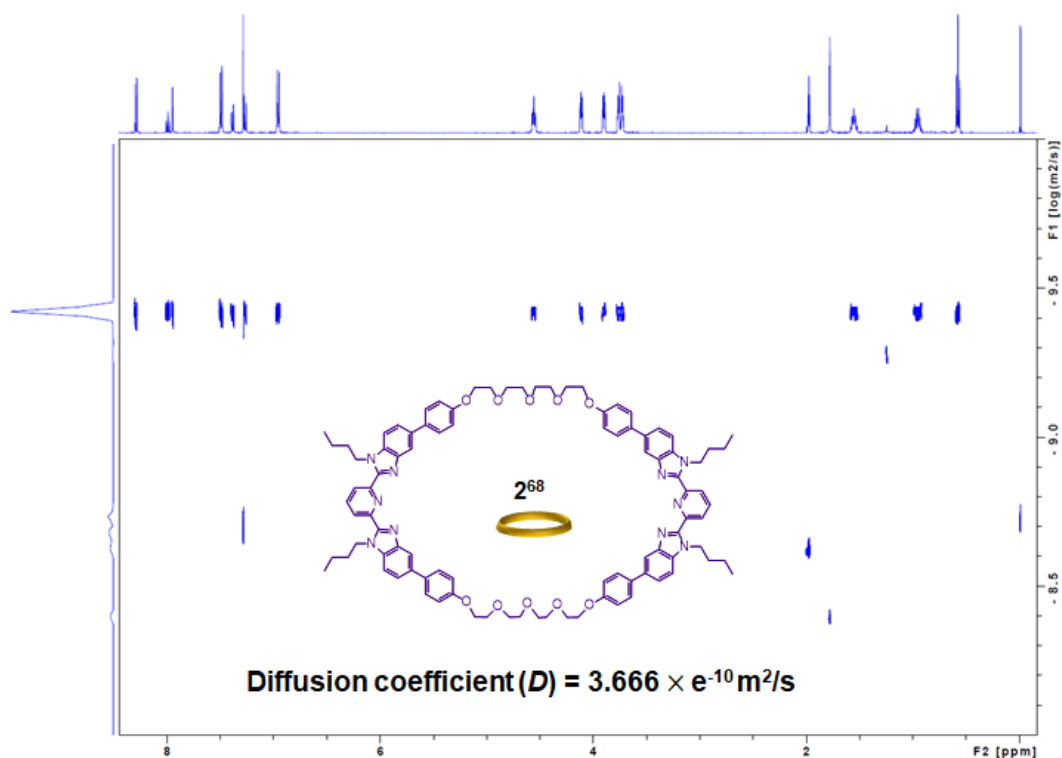


Figure S35. DOSY Spectrum (500 MHz, 25°C) and diffusion coefficient of 5mM of **2⁶⁸** (Solvent: 5% acetonitrile-*d*₃ in chloroform-*d*).

Reference

- [1] B. M. McKenzie, A. K. Miller, R. J. Wojtecki, J. C. Johnson, K. A. Burke, K. A. Tzeng, P. T. Mather, S. J. Rowan, *Tetrahedron* **2008**, *64*, 8488-8495.
- [2] Q. Wu, P. M. Rauscher, X. Lang, R. J. Wojtecki, J. J. De Pablo, M. J. Hore, S. J. Rowan, *Science* **2017**, *358*, 1434-1439.
- [3] J. E. Hertzog, V. J. Maddi, L. F. Hart, B. W. Rawe, P. M. Rauscher, K. M. Herbert, E. P. Bruckner, J. J. de Pablo, S. J. Rowan, *Chem. Sci.* **2022**, *13*, 5333-5344.
- [4] A. Jerschow, N. Müller, *J. Magn. Reson.* **1996**, *123*, 222-225
- [5] A. Jerschow, N. Müller, *J. Magn. Reson.* **1997**, *125*, 372-375.
- [6] *Bruker Topspin 1D and 2D Experiments Step-by-step Tutorial; Advanced Experiments User Guide* **2006**.
- [7] H. Teisala, P. Baumli, S. A. L. Weber, D. Vollmer, H.-J. Butt, *Langmuir* **2020**, *36*, 4416-4431.
- [8] P. Ziegler, *Bruker Topspin Advanced NMR Methods User Manual*, **2010**.
- [9] K. Zhang, W. Feng, C. Jin, *MethodsX* **2020**, *7*, 100779.